JOURNAL OF GEOPHYSICAL RESEARCH, VOL. 107, NO. B12, 2331, doi:10.1029/2001JB000308, 2002

Arc parallel extension and localization of volcanic complexes in Guadeloupe, Lesser Antilles

N. Feuillet,[1] I. Manighetti, and P. Tapponnier

Institut de Physique du Globe de Paris, Laboratoire de Tectonique et Mécanique de la Lithosphère, CNRS UMR 7578, Paris, France

E. Jacques

Institut de Physique du Globe de Strasbourg, France

Received 8 August 2000; revised 13 December 2001; accepted 18 December 2001; published 7 December 2002.

[1] Subduction of Atlantic seafloor under the Caribbean plate causes shallow earthquakes within the Lesser Antilles volcanic arc. Such earthquakes, above the subduction interface, show strike-slip or normal fault plane solutions, the latter with ~E-W striking nodal planes. To better assess seismic hazard and the coupling between volcanism and tectonics, we investigated faulting related to overriding-plate deformation in the Guadeloupe archipelago. Using aerial photographs, satellite SPOT images, and topographic maps (1/25000 scale), we mapped active and middle to late Pleistocene fissures and normal fault systems that cut the uplifted coral platforms Grande-Terre and Marie-Galante and the volcanic rocks of Basse-Terre. The available marine geophysical data show that the faults extend offshore to bound submarine rifts. The E-W striking, 1500 m deep, V-shaped Marie-Galante rift separates the two islands of Marie-Galante and Grande-Terre. Normal faults in the north of Grande-Terre appear to mark the similarly V-shaped, western termination of the 5000 m deep, N°50E to N130°E striking Desirade graben. Three shallow, M ~ 5.5 earthquakes (6 May 1851, 29 April 1897, 3 August 1992) appear to have ruptured segments of the Marie-Galante rift boundary faults. The young "La Grande Découverte" volcanic complex of Basse-Terre, including the 1440 A.D. Soufrière dome, lies within the western termination of the Marie-Galante rift. The ancient volcanic shoulders of the rift buttress the active dome to the north and south, which may explain why major prehistoric sector collapses and pyroclastic avalanches have been directed southwestward into the Caribbean Sea, or southeastward into the Atlantic Ocean. The Marie-Galante rift is typical of other troughs transverse to the northeastern edge of the Caribbean plate. We interpret such troughs, which are roughly orthogonal to the arc, to result from slip-partitioning and extension perpendicular to plate convergence. That they disappear southward implies that they result from interaction between the Caribbean and North American plates. *INDEX TERMS:* 7230 Seismology: Seismicity and seismotectonics; 8010 Structural Geology: Fractures and faults; *KEYWORDS:* Lesser Antilles, Guadeloupe, seismic and volcanic hazards, active faulting, arc-parallel extension, seismicity

Citation: Feuillet, N., I. Manighetti, P. Tapponnier, and E. Jacques, Arc parallel extension and localization of volcanic complexes in Guadeloupe, Lesser Antilles, *J. Geophys. Res.*, *107*(B12), 2331, doi:10.1029/2001JB000308, 2002.

1. Introduction

[2] The eastern edge of the Caribbean plate is best known as a site of volcanic hazard. In 1902, for instance, the Montagne Pelée eruption wiped out the town of Saint Pierre, in Martinique, killing 30,000 people. Since 1996, the still ongoing eruption of the Soufriere Hills of Montserrat has devastated the better part of that island. But the Caribbean arc is also an area of serious seismic hazard. Historically, several large ($M \geq 7$) earthquakes have been recorded (5 April 1690, Nevis; 8 February 1843, Guadeloupe; 18 November 1867, Virgin Islands; 8 October 1974, Antigua), some apparently rupturing the plate interface (e.g., 1843 [*Bernard and Lambert*, 1988]), and others intraplate normal faults (e.g., 1974 [*McCann et al.*, 1982]). In this paper, we seek to improve understanding of recent tectonics and related seismic and volcanic activity in the northern Lesser Antilles arc. Specifically, we try to determine which faults might be responsible for the shallow seismicity within the arc, and to understand their origin. We also examine the links between shallow faulting and vol-

[1]Now at Istituto Nazionale di Geofisica e Vulcanologia, Rome, Italy.

0148-0227/02/2001JB000308$09.00

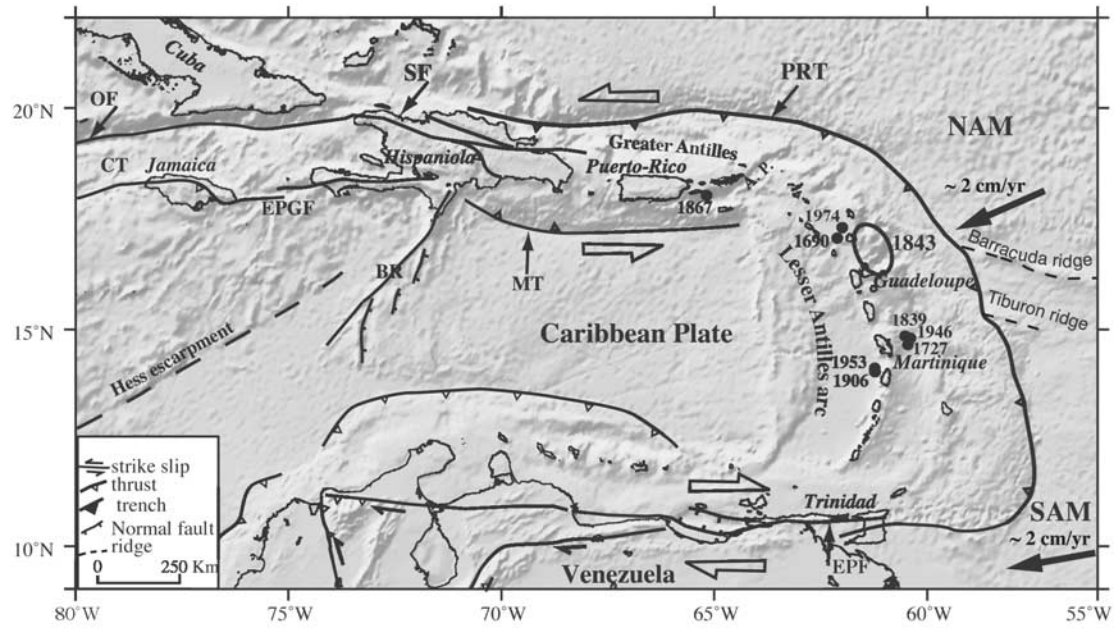

Figure 1a. Geodynamic setting of Lesser Antilles arc [after, e.g., *Jordan*, 1975; *Adamek et al.*, 1988; *Holcombe et al.*, 1990; *Mascle and Letouzey*, 1990; *Pindell and Barrett*, 1990; *Heubeck and Mann*, 1991; *Mann et al.*, 1995; *Flinch et al.*, 1999; *Weber et al.*, 2001]. Bathymetry from *Smith and Sandwell* [1997]. Subduction rates from *DeMets et al.* [2000] and *Weber et al.* [2001]. CT: Cayman Trough, OF: Oriente Fault zone, EPGF: Enriquillo-Plantain Garden fault zone; BR: Beata Ridge; MT: Muertos trough, PRT: Puerto Rico trench, EPF: El Pilar Fault zone. Black circles: major historical earthquakes ($I \geq$ VIII–IX, $M > 7$) in the Lesser Antilles arc with dates after *Robson* [1964]; *Feuillard* [1985]; *Bernard and Lambert* [1988]. The patch ruptured by the 1843 earthquake is indicated.

canism. Our main focus is a detailed neotectonic study of the Guadeloupe archipelago, which is composed of three calcareous islands, La Désirade, Marie-Galante and Grande-Terre, and one volcanic island (Basse-Terre), site of the active Soufrière volcano.

[3] Using available topographic, bathymetric and geological evidence, combined with measurements in the field, we first document the geometry and kinematics of Quaternary faulting across the four islands, both onland and offshore. Panchromatic and XS SPOT satellite images (1/50000 scale), stereoscopic air photographs (1/20000 scale), and digital elevation models (horizontal resolution of 50 m), are used to map faults cutting recent volcanic or reef surfaces and exhibiting youthful morphology. Topographic profiles (from topographic maps (1/25000 scale) or DEMs), perpendicular to the faults, are used to determine large-scale block-tilting and the shapes, maximum slopes and heights of cumulative scarps. The detailed geometry of fault scarps (strike, segmentation, bends, steps) is studied in map view to obtain information on fault kinematics. Field observations and microtectonic measurements (e.g., slickensides, offsets) are combined to characterize such faults down to scales of a few meters. In the submarine part of the archipelago, we use the bathymetry to identify faults that continue underwater and further constrain their geometry. Submarine faults scarps are mapped using perturbations of bathymetric gradients. Steep gradients between slope breaks allow fault throws to be estimated from orthogonal profiles. Extant marine seismic profiles help constrain the geometry and throw of the faults at depth.

[4] Based on the entire data set, we discuss the relationships between volcanism and faulting. Finally, we critically assess the historical seismicity in the framework of our tectonic study, and the origin of Quaternary faulting in the northern Lesser Antilles arc.

2. Tectonic Setting of the Lesser Antilles Arc

[5] Along the northern Lesser Antilles arc, the North American and Caribbean plates converge in a roughly ENE direction, at a rate now known to be 2 cm/yr (Figure 1) [*Deng and Sykes*, 1995; *Dixon et al.*, 1998; *DeMets et al.*, 2000]. This motion is chiefly absorbed by subduction of Atlantic seafloor under the arc (Figure 1a). The Caribbean plate is bounded to the north by the North American-Caribbean plate boundary zone, a 100- to 250-km-wide, >2000-km-long, seismogenic zone with mainly left-lateral, strike-slip deformation. This zone is limited to the north by the Oriente and Septentrional faults and the Puerto Rico trench, and to the south by the Motagua-Polochic, Swan Islands, Enriquillo-Plantain Garden faults and the Muertos trough. To the south, in northern Venezuela and Trinidad, the Caribbean plate is bounded by a dextral strike-slip fault zone, the El-Pilar-Central Range fault zone [e.g., *Jordan*, 1975; *Adamek et al.*, 1988; *Holcombe et al.*, 1990; *Mascle and Letouzey*, 1990; *Pindell and Barret*, 1990; *Heubeck and Mann*, 1991; *Mann et al.*, 1995; *Flinch et al.*, 1999; *Weber et al.*, 2001]. The subduction zone is strongly curved between these two strike-slip boundaries. The Lesser Antilles arc roughly parallels the trench, 200 to 400 km to the west (Figure 1). It is ~850 km

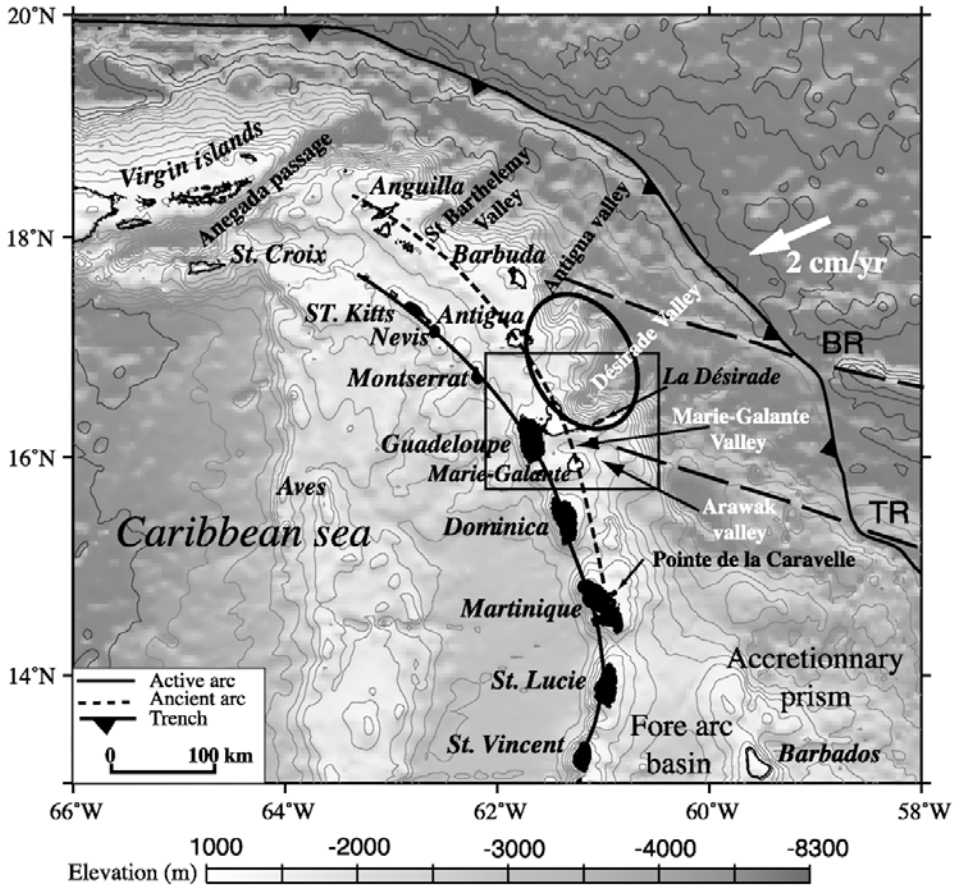

Figure 1b. Bathymetric map of Lesser Antilles arc. Bathymetry from *Smith and Sandwell* [1997], contour interval, 500 m. Continuous black line, recent volcanic arc; dotted black line, ancient arc after, e.g., *Bouysse et al.* [1988]. Volcanic islands (on recent arc) in black; coral reef islands (on ancient arc) in white. Box indicates location of Figure 14a. Black dashed lines mark Barracuda (BR) and Tiburon ridges (TR) (from *Feuillet et al.* [2001], reprinted from *Comptes rendus de l'Académie des Sciences, Serie II, Sciences de la Terre et des Planètes*, with permission from Elsevier Science).

long between the Anegada passage and the Venezuelan coast, and made of a dozen volcanic islands. The overall bathymetry [*Smith and Sandwell*, 1997] (Figure 1b) shows that, north of ~14°30′N, the arc is divided by the Kallinago basin into two subparallel ridges that splay from the island of Martinique. The western one is made of volcanic islands, most of them with active volcanoes ("volcanic Caribbees," black in Figure 1b [e.g., *Bouysse*, 1979; *Bouysse et al.*, 1985, 1988; *Bouysse and Westercamp*, 1990]). The shorter eastern one, 10 to 50 km to the east, is composed of islands with an old basement overlain by uppermost Miocene and Plio-Quaternary coral limestones ("limestone Caribbees," white in Figure 1b). Although the origin of the Kallinago basin, which wedges out north of Martinique's Caravelle Peninsula is poorly known, the division of the arc may result from kinematic changes in the subduction process [*Bouysse and Westercamp*, 1990].

[6] The northeastern part of the arc is cut by bathymetric troughs at high angle to the trench, the longest and deepest being the Anegada passage, between the Lesser and the Greater Antilles (Figure 1b). Some of these troughs have been interpreted to result from normal faulting within the Caribbean plate [*Tomblin*, 1972; *Case and Holcombe*, 1980; *Stefan et al.*, 1985]. One fault segment along the Anegada trough may have produced the disastrous 1867, 7.5 M_s, Virgin Islands earthquake [*McCann*, 1985].

[7] The distribution of historical and instrumental earthquakes throughout the arc attests to widespread intra and interplate seismic activity, particularly in the north where recorded events are more numerous and where the strongest shocks ($mb \geq 6$) have occurred [*Robson*, 1964; *Sykes and Ewing*, 1965; *Dorel et al.*, 1971; *Dorel*, 1981; *Stein et al.*, 1982; *Feuillard*, 1985; *Bernard and Lambert*, 1988; *Dziewonski et al.*, 2000] (see also on-line catalogs from International Seismological Centre (ISC), Thatcham, United Kingdom; National Earthquake Information Service (NEIS), National Earthquake Information Center, U.S. Geological Survey; and Harvard University, available at http://www.isc.ac.uk/Bull; http://neic.usgs.gov/neis; and http://www.seismology.harvard.edu/CMTsearch.html, respectively) (Figure 2a). Overall, hypocenter depths increase westward, from a few kilometers near the trench down to ~220 km in the subducted slab beneath the western arc [*Dorel*, 1981] (Figure 2). The plate interface dips at a shallow angle west of the trench and much more steeply under the arc with a marked flexure offshore the outer islands (Figure 2b).

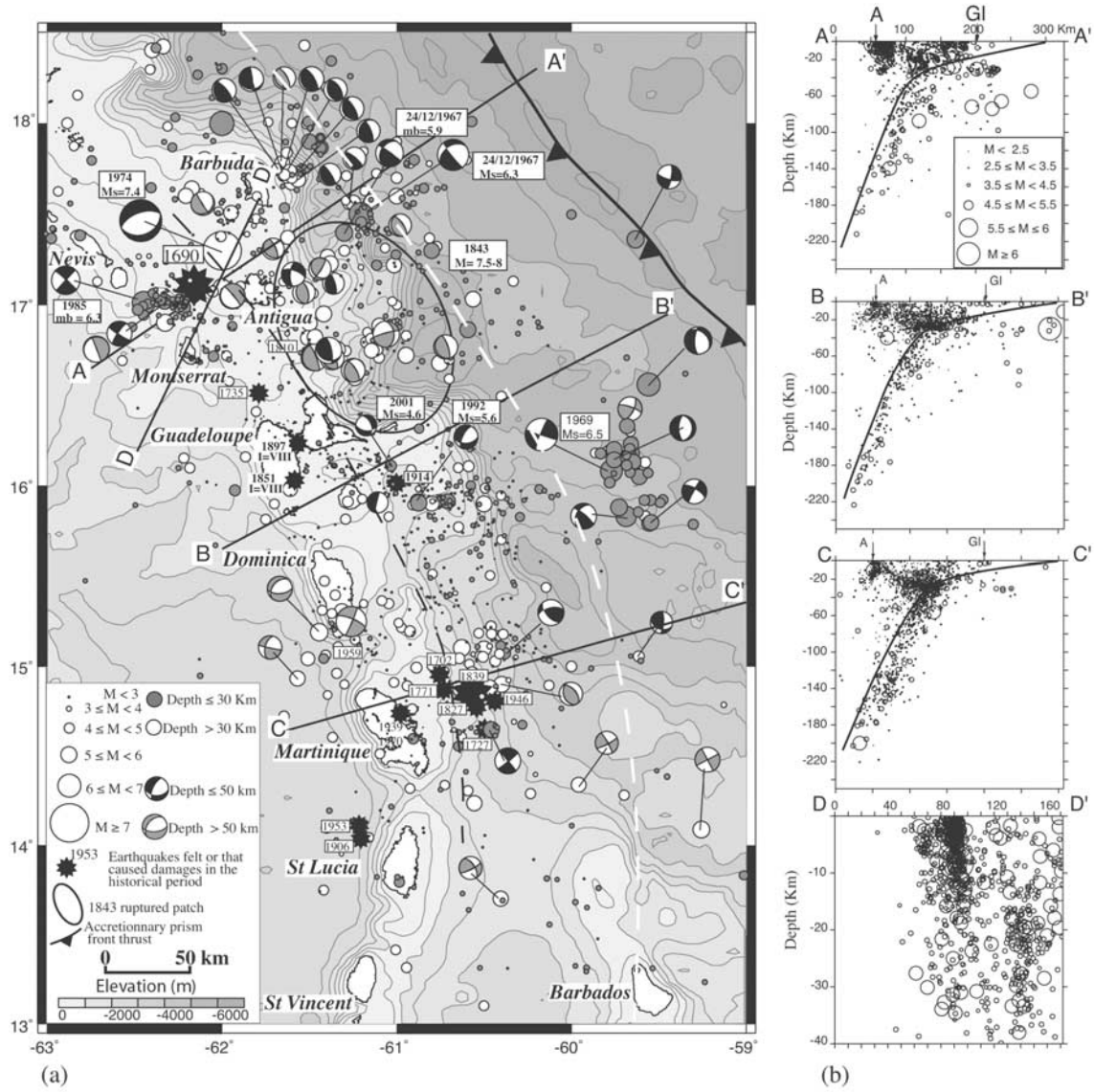

Figure 2. (a) 1950–2001 seismicity in Lesser Antilles arc. Historical seismicity and focal mechanisms are from *Robson* [1964], *Stein et al.* [1982], *Feuillard* [1985], *Bernard and Lambert* [1988], and *Dziewonski et al.* [2000] (see also on-line catalogs from International Seismological Centre (ISC), Thatcham, United Kingdom; National Earthquake Information Service (NEIS), National Earthquake Information Center, U.S. Geological Survey; and Harvard University, available at http://www.isc.ac.uk/Bull; http://neic.usgs.gov/neis; and http://www.seismology.harvard.edu/CMTsearch.html, respectively). Overall, depths of events increase westward, in agreement with slab geometry and dip; however, shallow seismicity spreads within whole arc. Many shallow earthquakes have normal (1974, 1992, 2001) or strike-slip (1985, 1967) mechanisms, and are related to intraplate deformation. Dates of major events are indicated in white boxes. Roman numerals: intensity of the 1851 and 1897 earthquakes. Dotted white line: gravimetric anomaly. Dotted black line: position of the Benioff zone at 50 km depth. (b) Distribution of regional seismicity recorded by Guadeloupe and Martinique regional networks (IPG), at depth, on vertical sections (location, Figure 2a). Informations on seismic networks can be found in annual reports of Observatories of Institut de Physique du Globe. Main seismic stations are located on Nevis, Antigua, Montserrat, Basse-Terre, Grande-Terre, Marie-Galante, La Désirade (9 stations, 3 are 3C), Dominica, Martinique, and Sainte-Lucie (8 stations, 3 are 3C). Fourteen and twelve additional seismometers (two 3C) are concentrated on the Soufrière and Montagne Pelée volcanoes, respectively. Most seismometers are analogic short period telemetered stations, except two Lennartz stations on La Désirade and Basse-Terre. A, arc; Gl, gravimetric anomaly. Deep seismicity underlines subducting slab, which keeps seismogenic down to 220 km depth, with a roughly constant dip along the arc. Approximate surface of slab is underlined by black lines. On DD′, the N135°E striking fault plane that ruptured during the 1985 sequence, near Montserrat island, is visible down to a depth of 15 km. See discussion in text.

In the north, several focal mechanisms indicate thrust events on NNW striking planes roughly parallel to the trench, generally with one nodal plane dipping at a shallow angle toward the arc (Figure 2a), and thus clearly related to subduction. In addition to seismicity reflecting the westward plunge of the slab, shallow shocks occur at crustal depths ($\leq$20–30 km) within the arc, particularly in the north. Although such shallow seismicity looks diffuse, a few areas show greater concentrations of earthquakes, such as north of Montserrat, NE of Antigua, NE of Guadeloupe, between Grande-Terre and Marie-Galante, south of Dominica, NE of Martinique. With the exception of shallow thrust earthquakes east of Barbuda, focal mechanisms calculated for the most superficial shocks in the arc tend to show either normal or strike-slip faulting on planes striking either roughly NW-SE, NE-SW, or E-W. The relationship, however, between shallow earthquakes and active faults remains, in general, poorly known.

3. Morphotectonic Analysis of Faulting in the Guadeloupe Archipelago

3.1. Faulting Onland

[8] The eastern part of the island of Guadeloupe (Grande-Terre) and the island of Marie-Galante (Figure 3a, inset) are chiefly made of fairly uniform Pleistocene reef limestones [*Andreieff et al.*, 1987; *Garrabé et al.*, 1988; *Bouysse et al.*, 1993], capping pre-Miocene volcanic basement [*Bouysse and Westercamp*, 1990; *Le Mouël et al.*, 1979; *Gérard et al.*, 1981]. In la Désirade, probably older, lower Pliocene reef limestones [*Westercamp*, 1980; *Andreieff et al.*, 1987] cap a more ancient Upper Jurassic [*Montgomery et al.*, 1992] or Lower Cretaceous [*Bouysse et al.*, 1983b] igneous basement, of debatable origin.

[9] The three islands form flat calcareous tables, rising tens to hundreds of meters above sea level. Due to weathering in the tropical environment, such tables are dissected by a network of valleys, and pitted by karstic dollines, whose density and size is greatest in ''Les Grands-Fonds'' (Grande-Terre), ''Morne Piton'' and ''Morne Constant'' (Marie-Galante). Both the flat limestone surfaces and the karstic drainage networks are cut and offset by continuous scarps which form steep, sharp steps in the morphology, up to 10 km long and 130 m high, between undisrupted areas. Usually, there are no rivers flowing along the base of such scarps, which therefore do not result from fluvial incision. Most of them bear hanging wineglass valleys, implying that transverse stream incision has not kept pace with relative tectonic uplift [*Wallace*, 1981; *Armijo et al.*, 1986]. The major scarps cut the present shorelines of the islands, whose cliffs usually expose steeply dipping fault planes beneath them. Besides, systems of subparallel, open fissures and clastic or calcite dykes often follow the scarps. These scarps thus mark the traces of active faults cutting the calcareous tabular surfaces of the islands of Grande-Terre, Marie-Galante and La Désirade. Below, we describe the main active faults on each island in greater detail (for even more complete descriptions, see *Feuillet* [2000]).

3.1.1. Grande-Terre

[10] The island of Grande-Terre encompasses three regions with different faulting geometries (Figure 3a).

[11] The northern part of the island is cut by three large, N10° ± 10°E striking, east facing fault scarps (Grande-Vigie/Caraïbe, Montagne Vercinot, Portland) that form clear steps in the topography, up to 10 km long and 70 m high. They divide the ''northern plateaus'' in NE elongated blocks (Hauteur Caraïbes, Saint Jacques and Mangles), tilted northwestward by ~1° (Figure 4a). The Grande-Vigie/Caraïbe fault cuts the sea cliff that rims the northern tip of Grande-Terre, exposing the relationship between the fault plane in section and the cumulative scarp profile in the morphology (Figure 5a). This plane dips 80° eastward and bears dip-slip slickensides that attest to pure normal slip (Figure 5b). It projects at the surface into a ~6-m-high scarplet whose slope is the steepest of the cumulative scarp profile. As commonly observed elsewhere, this steepest part of the scarp, whose base runs along the top of the colluvial wedge near the inflexion point of the scarp profile, is the surface record of the last earthquake ruptures on the fault [*Wallace*, 1981; *Armijo et al.*, 1986; *Avouac and Peltzer*, 1993; *Benedetti et al.*, 1999]. Although they are clearly active and show the highest scarps, the ~N10° ± 10°E striking normal faults are at places cut by smaller, N165°E striking faults. Thus both fault systems are currently active. The left stepping segmentation of the latter is suggestive of normal right lateral slip.

[12] The southern part of Grande-Terre is also cut by active normal faults, but their orientation is different (N70°–130°E). Most of them are located near the southern shore of the island, between Pointe-à-Pitre and the ''Pointe des Chateaux'' where they cut the sea cliff (Figure 5c). Their scarps face southward, have lengths up to ~15 km and heights up to 60 m. They tilt northward the eastern plateaus of Grande-Terre by about 0.5° (Figure 4b) and truncate hanging valleys. The Gosier fault, that bounds to the south the Grands-Fonds region, is the longest and highest of these faults. To the west, the hanging wall at the base of its scarp and the lowest parts of transverse, antecedent valleys on the footwall have been flooded by the Holocene sea, then covered by recent clay deposits [*Garrabé et al.*, 1988]. South of the central stretch of the Gosier fault, another south dipping normal fault bounds the coast, uplifting the village of Gosier by more than 30 m. The overall geometries of the southern faults reveal variable kinematics. Faults striking on average N90° ± 10°E have continuous traces and the highest vertical throws. Some of them pair to bound grabens such as the flat floored ''Vallée d'Or'' (Figure 5d) or that at ''Pointe Tarare'' (Figures 5g and 5h) whose floor is cut by N90°–120°E striking open fissures (Figure 5f). This attests to pure normal slip on the N90° f± 10°E striking faults and to ongoing ~N-S extension. Most faults striking N120° ± 10°E (as the Fond-St-Bernard fault) are composed of right stepping segments, indicating a left-lateral component of slip. This is confirmed by slickenside measurements made on the Bragelone fault plane (Figure 3b) exposed in a quarry (Figure 5e). By contrast, most faults striking ~N80 ± 10°E (as the Roche de May fault) are composed of left stepping segments, attesting to a right-lateral component of slip. Faults with different strikes commonly connect to one another. For instance, the Bragelone fault scarp height increases by ~20 m due east of its junction with the Roche de May fault scarp (Figure 3b), consistent with slip transfer between coeval normal faults.

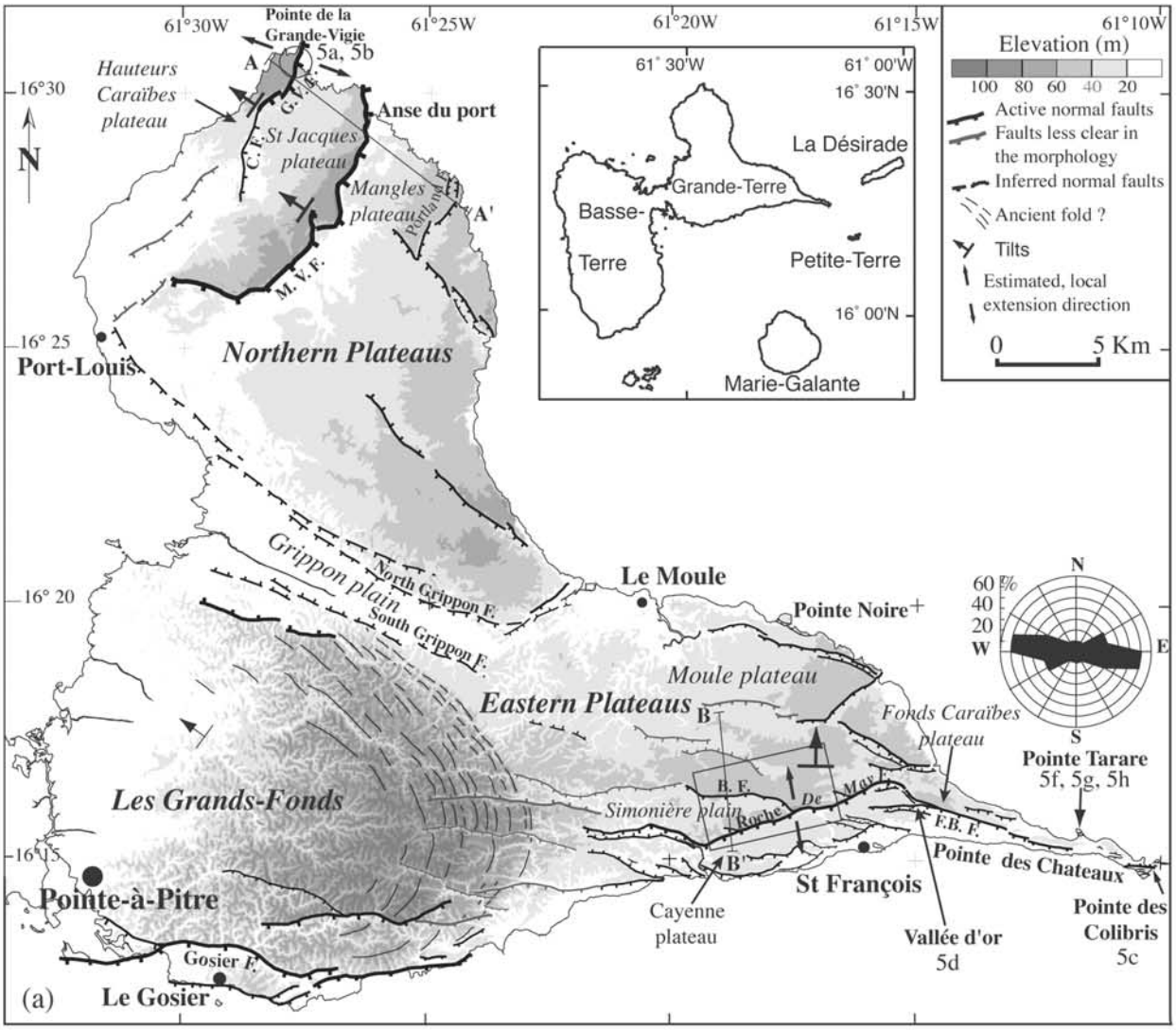
61°30W
61°25W
61°20W
61°15W
61°10W
16°30
16° 25
16° 20
16° 15
N
Pointe de la Grande-Vigie
5a, 5b
A
A'
Hauteurs Caraïbes plateau
G.F.
C.F.
St Jacques plateau
Anse du port
Mangles plateau
Portila F.
M.V.F.
Port-Louis
Northern Plateaus
Grippon plain
North Grippon F.
South Grippon F.
Le Moule
Pointe Noire
Moule plateau
Eastern Plateaus
B
B'
Fonds Caraïbes plateau
Pointe Tarare
5f, 5g, 5h
B. F.
De
May
Roche
Simonière plain
F.B. F.
Pointe des Chateaux
Les Grands-Fonds
Pointe-à-Pitre
St François
Cayenne plateau
Vallée d'or
5d
Pointe des Colibris
5c
Gosier F.
Le Gosier
(a)
61° 30'W
61° 00'W
16° 30'N
16° 00'N
La Désirade
Grande-Terre
Basse-Terre
Petite-Terre
Marie-Galante
Elevation (m)
100 80 60 40 20
Active normal faults
Faults less clear in the morphology
Inferred normal faults
Ancient fold ?
Tilts
Estimated, local extension direction
0 5 Km
60 %
40
20
W
E
S

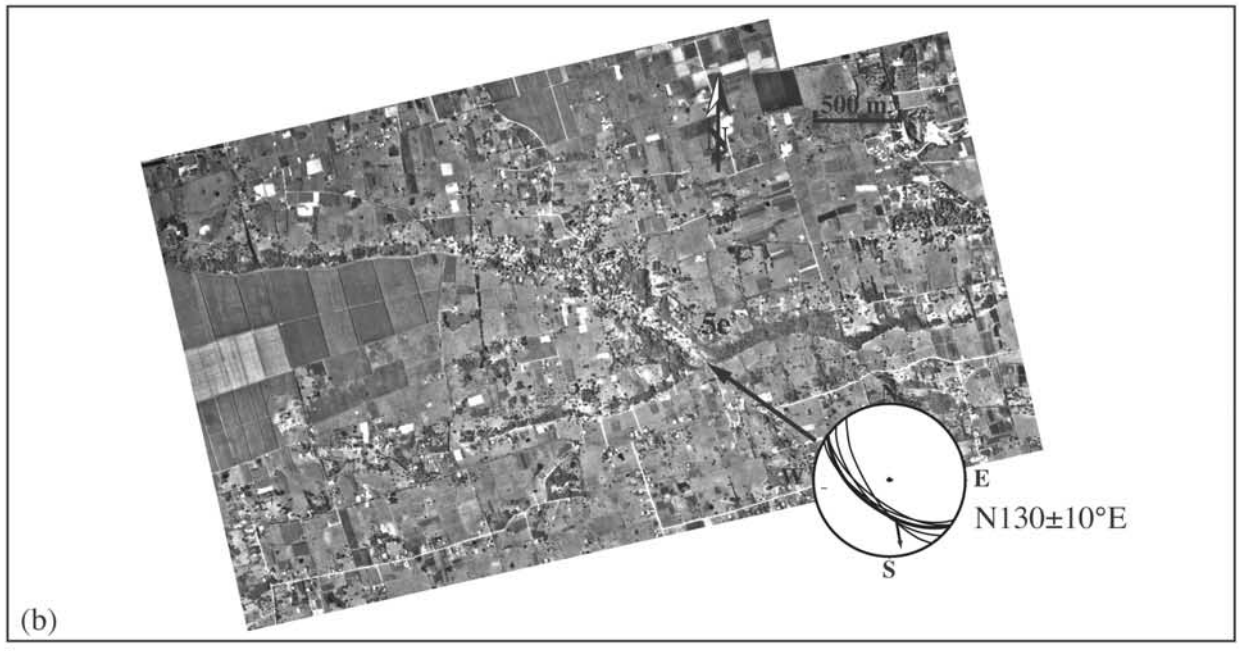
500 m
5e
W
E
S
N130±10°E
(b)

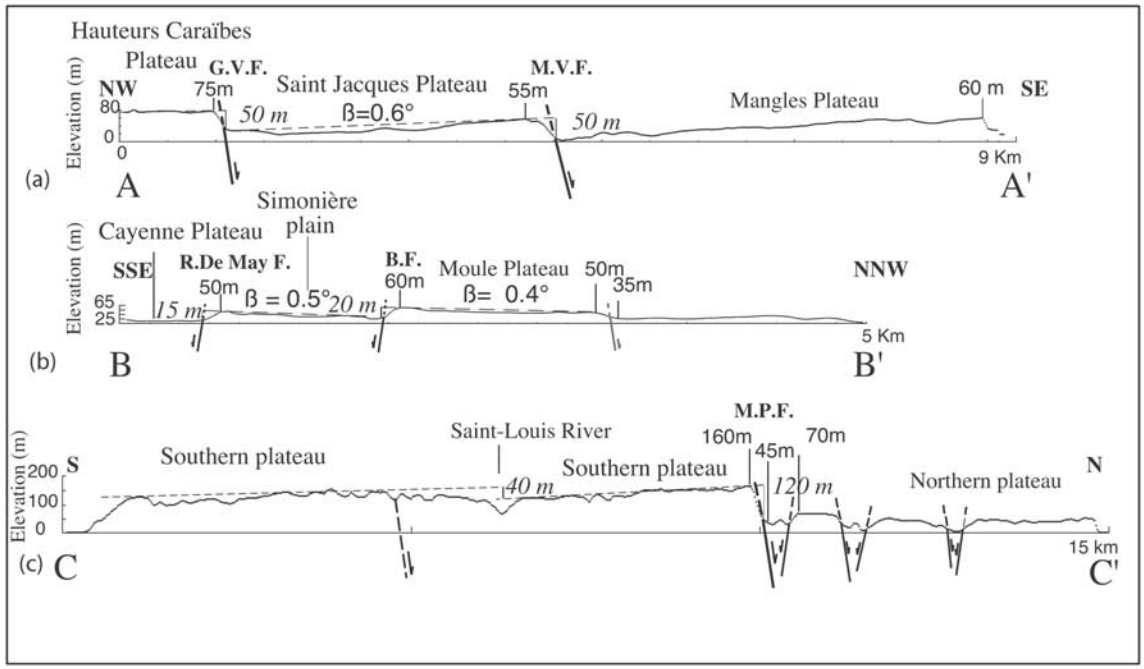

Figure 4. Morphological and tectonic interpretation of topographic sections across Guadeloupe islands. Sections are extracted from DEM. AA′, and BB′ across northern and eastern plateaus of Grande-Terre, respectively (location in Figure 3a); CC′ across Marie-Galante (location in Figure 8a). Vertical exaggeration: 4. Normal faults are represented with steep solid lines, with arrows indicating hanging wall slip. Fault names as in Figure 3a; M.P.F for Morne-Piton fault. Standard numbers are elevations; numbers in italic are cumulative vertical throws. Thin dashed lines outline tilted surfaces, with β being tilt amount.

[13] The Grands-Fonds region, highest part of Grande-Terre, has an elliptical shape reflecting that of its volcanic basement [*Bouysse and Garrabe*, 1984], as suggested by magnetic and areomagnetic data [*Le Mouël et al.*, 1979; *Gérard et al.*, 1981]. Well-developed karstic erosion [e.g., *De Reynal de Saint Michel*, 1961] indicates that the Grands-Fonds permanently rose above sea level before the rest of the island [*Bouysse and Garrabe*, 1984]. Such intense erosion and weathering make active fault mapping more difficult. However, several ~E-W trending scarps, whose linearity contrasts with the complex local morphology, crosscut the labyrinth of karstic depressions. Some, which cut the subparallel ridges that rim the curved, eastern side of the Grands-Fonds, clearly correspond to the westward extensions of the faults mapped across the eastern plateaus. The origin of the ridges is unclear. They might be remnants of old shorelines or bending warped by more ancient folding as suggested by *Lasserre* [1961].

[14] The degraded and incised ridges that bound the clay mantled Grippon plain, probably follow two antithetic, N110°E striking normal faults limiting a graben (''north and south Grippon faults''), but their much weathered morphology indicates they are not active anymore.

3.1.2. La Désirade

[15] La Désirade forms a narrow, elongated plateau, tilted northward by ~1.5°–2.5°, shaped by two sets of oblique, interacting normal faults (Figure 6a). The northwestern edge of the plateau forms a 200-m-high, indented sea cliff. The southeastern edge, which is preserved from wave cutting by

Figure 3. (opposite) (a) Topographic and tectonic map of Grande-Terre island (Guadeloupe). Topography is from topographic maps (1/25 000 scale, Institut Géographique National). Fault identification and mapping are based on analysis of aerial and satellite images, topographic maps and fieldwork. Fault scarps with clearest morphological evidence of recent activity are in black, with thicker traces for higher scarps; less clearly active faults in grey; inferred faults in dashed lines with ticks; see discussion in text. Dashed curved lines: ridges. ''F'' for faults: G.V., Grande-Vigie, C., Caraïbes; M.V., Montagne Vercinot; B., Bragelone; F.B., Fond Saint Bernard. Full, double arrows: local directions of extension deduced from microtectonic measurements. Half arrows with bars: tilt of carbonate platform. Open circle: location of Figures 5a and 5b. Box: location of Figure 3b. Polar diagram of percentages of cracks with a given strike measured in site of Figure 5f is shown. Locations of topographic sections AA′, BB′ of Figure 4 are indicated. Inset: the islands of Guadeloupe archipelago. (b) Aerial photograph mosaic of Bragelone and Roche de May faults connection zone. Arrows indicate location of Figure 5e. Lower hemisphere equal area projection of fault planes measured in a quarry at the junction between Bragelone and Roche de May faults is shown.

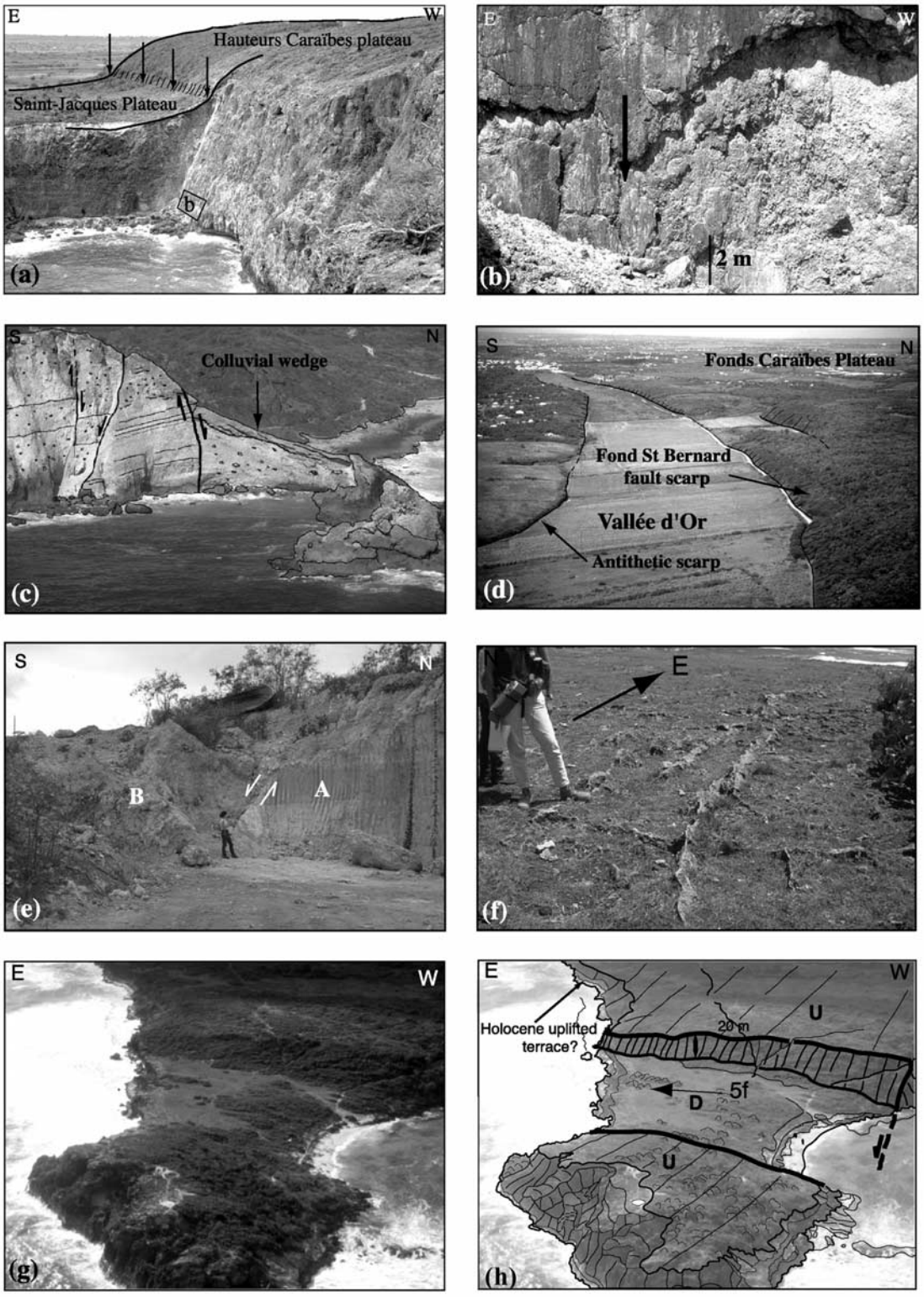
E
W
Hauteurs Caraïbes plateau
Saint-Jacques Plateau
b
(a)
E
W
2 m
(b)
S
N
Colluvial wedge
(c)
S
N
Fonds Caraïbes Plateau
Fond St Bernard
fault scarp
Vallée d'Or
Antithetic scarp
(d)
S
N
B
A
(e)
N
E
(f)
E
W
(g)
E
W
Holocene uplifted
terrace?
20 m
U
D
5f
U
(h)

fringing reefs, is more linear and bounded by a series of ~N50° ± 10°E striking, southeast dipping normal faults. These faults are cut by four major E-W striking, south facing normal fault scarps, the largest (Desert) being ~150–200 m high. The Desert fault extends offshore and offsets the fringing reef barrier to the east. Despite the crosscutting relationships, both fault systems exhibit comparably youthful escarpments suggesting coeval ongoing slip. In a quarry near Les Galets, these interacting faults can be observed at smaller scale, cutting lower Pliocene, NW tilted reef limestones [*Westercamp*, 1980]. At Pointe des Colibris (Figure 6b and inset) the Eemieen (119 ± 9 ka) coastal reef terrace, only a few meters above sea level [*Battistini et al.*, 1986], is cut by a ~150-m-long array of open fissures associated with small normal fault scarplets. The main fissures and faults stretch in a N65° ± 10°E direction, with up to several tens of centimeters of opening and of vertical throw respectively. Smaller N90° to 140°E striking fissures connect locally to the major one, at both ends. Thus, at all scales, open fissuring and normal faulting in La Désirade attest to current ~N-S extensional strain, mostly on coeval N60° ± 20°E and N100° ± 10°E striking planes.

3.1.3. Petite-Terre

[16] The twin islands of Petite Terre, ~10 km SE of Pointe Des Chateaux, form two flat reef platforms, elongated ~E-W (Figure 7). The smallest island (Terre de Haut), triangular-shaped, stands only 3 to 5 m above sea level. Its eastern and southern coasts are limited by sharp, straight cliffs. Terre de Bas, rectangular-shaped, is four times larger, and stands 1 to 12 m above sea level. Its highest part lies along its southeast coast. This coastline forms a sharp, steep cliff, contrasting with the northern coast, flooded by swamps. The morphology of the two islands suggests that both are tilted blocks, bounded to the south by two E-W striking normal faults. Open cracks cut corals and recent beach-rocks on both islands. The principal ones, along the islands southern coasts, have E-W strikes on average, with openings of up to 15–20 cm. They are associated with fissures striking either ~N110°E or N0°–25°E, with particularly prominent ones showing up to 30 cm of opening.

3.1.4. Marie-Galante

[17] The island of Marie-Galante is round-shaped, as an old volcano abraded by the sea (Figure 8a). It is fairly flat and capped by the broadest high reef plateau of the archipelago, reportedly of Pleistocene age [*Andreieff et al.*, 1987; *Grellet et al.*, 1988]. The plateau is divided into two parts, separated by the Morne Piton fault, a long recognized feature also called "Barre de l'île" [e.g., *Lasserre*, 1961; *Chabellard*, 1986] (Figure 9a). With a length of ~15 km and a height everywhere in excess of 60 m, the Morne-Piton scarp, that offsets both shores of the island, is the most important active fault escarpment in the whole Guadeloupe archipelago. It forms a steep, continuous, north facing step, whose strike varies between N90° and 140°E from east to west. The Morne-Piton fault lowers the northern plateau, whose mean elevation is 50 m, by usually more than 100 m (up to 130 m at places) relative to the southern plateau, which stands 150 m above sea level (Figure 8a). The southern plateau is tilted southward by ~0.4° (Figure 4c). The Morne-Piton scarp exhibits a succession of hanging wine-glass valleys (Figure 9a), a morphology that typifies active normal faults [e.g., *Wallace*, 1981; *Armijo et al.*, 1986]. At both ends, the Morne-Piton fault splays into shorter, synthetic, ~N60° to N90°E striking normal faults. Some of these faults, that strike on average N60 ± 10°E, with several of them dipping southward, are observed in section, at Anse-Piton, where they offset the basal interface between the reef limestones and the underlying volcanics (Figures 8a and 9b). In contrast with the southern plateau which is faulted only by an ~E-W, ~40-m-high fault scarp with smoothed out morphology south of the Saint Louis river, the northern plateau is cut by numerous recent normal faults (Figure 8a). Several of these faults pair to bound small ~E-W to N60°E trending grabens, all of which merge toward the southwest with the NW striking part of the Morne-Piton fault. Such a geometry, which resembles a

Figure 5. (opposite) Field views of some of the main Quaternary normal faults and fissures in Guadeloupe archipelago (location, Figure 3). (a) Southwestward view of Grande Vigie fault, which can be seen both offsetting the Quaternary reef surface and in cross section in the cliff; arrows indicate scarp emergence at the surface; location of Figure 5b is indicated. Tick marks underline the steepest ~6 m high scarplet related to the last earthquake ruptures on the fault (see text) (from *Feuillet et al.* [2001], reprinted from *Comptes rendus de l'Académie des Sciences, Serie II, Sciences de la Terre et des Planètes*, with permission from Elsevier Science). (b) Vertical slickensides on Grande Vigie fault plane (location in Figure 5a); black arrow marks slickenside pitch, which attests to pure dip slip motion on the fault (from *Feuillet et al.* [2001], reprinted from *Comptes rendus de l'Académie des Sciences, Serie II, Sciences de la Terre et des Planètes*, with permission from Elsevier Science). (c) Westward view of Pointe des Colibris. A steep, E-W striking, north dipping, normal fault offsets the topography and tilts calcareous beds southward. Its hanging wall is covered by a colluvial wedge; its footwall is cut by secondary, synthetic and antithetic faults. (d) Westward view of the Vallée d'Or graben, filled with Late Quaternary clay deposits. (e) Westward view of Bragelone fault in a quarry near its junction with the Roche-De-May fault. The main fault plane strikes N126°E, dips 57° to the southwest and bears downdip slickensides with a 60°SE pitch. It juxtaposes two Pleistocene limestones, a fine one (A) to a coarser one containing coral fragments (B) and is associated to smaller faults striking N120 to 145°E and dipping ~65° southwestward. White half arrows: motion along the plane. Scale given by the first author. (f) Eastward view of extensional crack network cutting Pointe Tarare graben inner floor. Location in Figure 5h. Cracks, filled with calcite, are mostly parallel to the E-W striking graben bounding faults (Figures 5g and 5h) and accommodate N-S extension, near the surface, between these faults. (g and h) Southward view of Pointe Tarare, fault bounded graben, and interpretation; U, uplifting footwall; D, downdropped graben floor. Note that southernmost footwall is rimmed by reef terraces or wave-cut notches of probably Holocene age, standing 1–2 m above sea level, which indicates current uplift of the footwall. Arrow indicates location of Figure 5f.

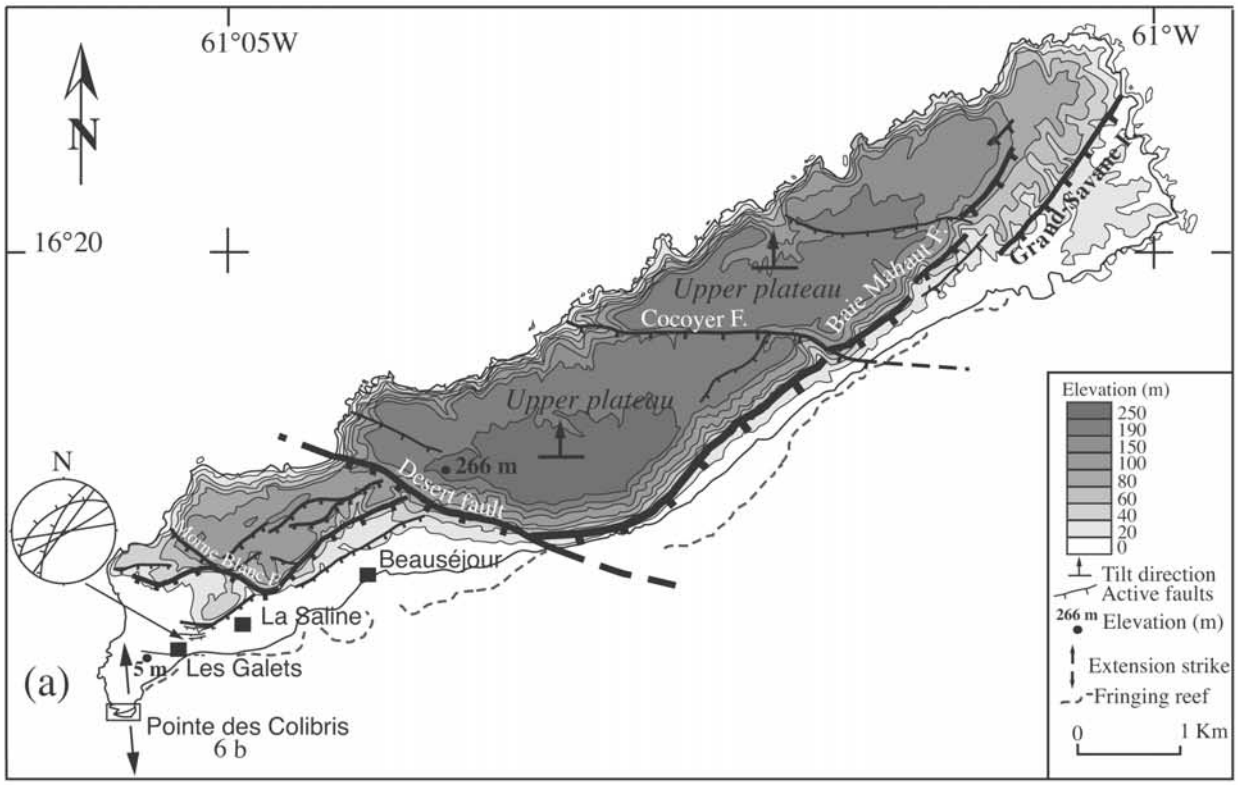
61°05W
61°W
16°20
N
Upper plateau
Cocoyer F.
Baie Mahaut F.
Grand-Savane F.
Upper plateau
266 m
Desert fault
Beauséjour
La Saline
5 m
Les Galets
Pointe des Colibris
6 b
(a)
Elevation (m)
250
190
150
100
80
60
40
20
0
Tilt direction
Active faults
266 m Elevation (m)
Extension strike
Fringing reef
0
1 Km

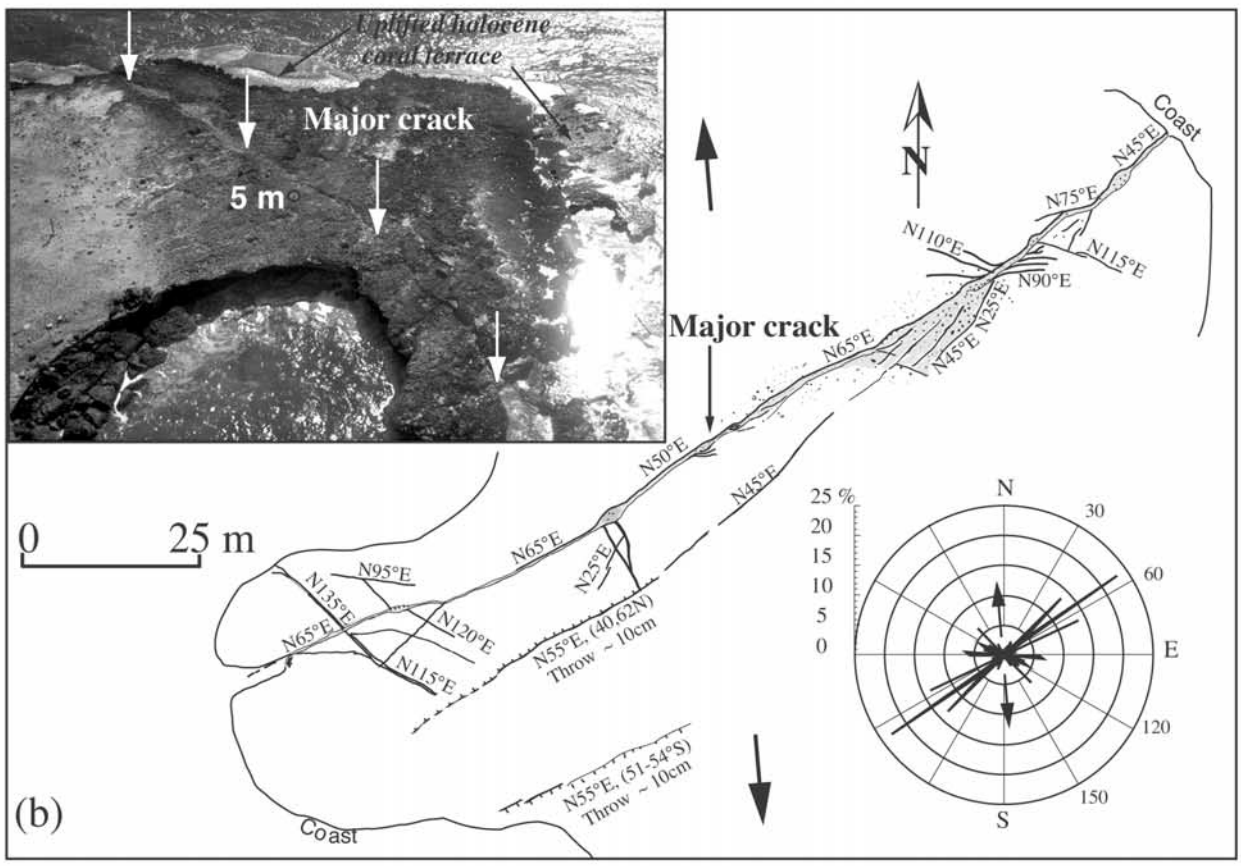
Uplifted holocene coral terrace
Major crack
5 m
Major crack
Coast
N45°E
N75°E
N110°E
N115°E
N90°E
N65°E
N45°E N25°E
N50°E
N45°E
N65°E
N25°E
N95°E
N135°E
N65°E
N120°E
N115°E
N55°E, (40,62N)
Throw ~ 10cm
N55°E, (51-54°S)
Throw ~ 10cm
0
25 m
25 %
20
15
10
5
0
N
30
60
E
120
150
S
(b)
Coast

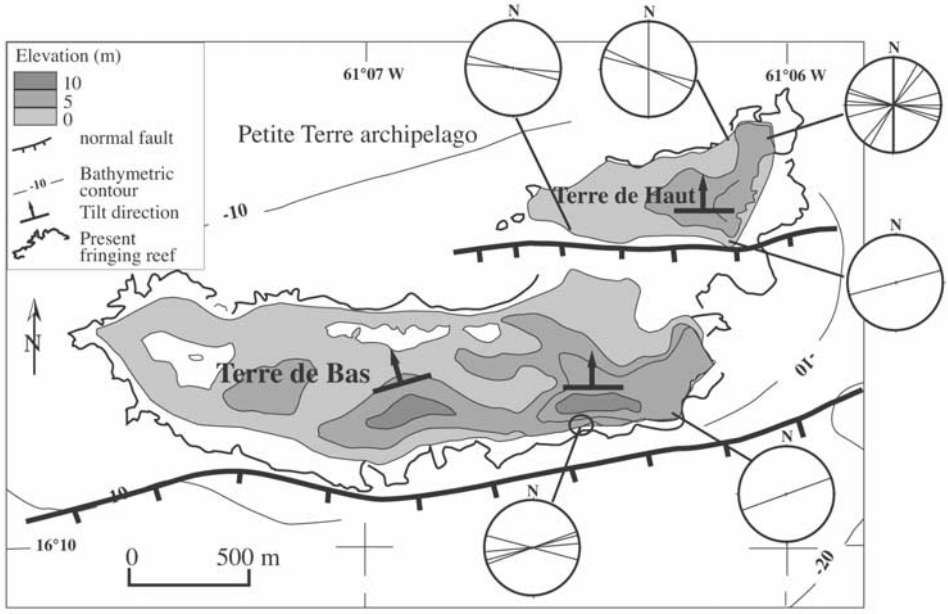

Figure 7. Topographic and structural map of Petite-Terre archipelago. Topography and symbols as in Figure 3a. Bathymetric contours from SHOM (Service Hydrographique et Océanographique de la Marine). Fringing reef, black line. Stereoplots show measured crack planes.

horsetail, suggests a left-lateral component of slip on this part of the Morne-Piton fault.

[18] That the Morne-Piton fault is active is confirmed by the sudden interruption of fringing coral reefs and marine terraces where the fault intersects the eastern coast of the island (Figure 8). South of Anse-Piton, the coast shows gentle shores lined with beaches and coral ledges [e.g., *Lasserre*, 1961; *Battistini et al.*, 1986; *Bouysse et al.*, 1993] (Figure 9c). North of Anse-Piton, the coastline is instead marked by an abrupt sea cliff. Using aerial photographs and topographic maps (1/20,000 and 1/25,000 scale, respectively), we mapped in detail three Quaternary reef terraces (Figure 8b). Immediately south of Anse-Piton, two principal terraces are identified. The highest (''Des Galets'') stands 50 m above sea level on average. The lowest one (''Capesterre''), which is only ~5 m above sea level on average, has been dated at 120 ka near Capesterre by the U-Th method [*Battistini et al.*, 1986]. An additional terrace (''Vavon'') extends locally between the other two, near the fault scarp. At Pointe Des Basses (Figure 8a), far to the south, the Capesterre terrace is only ~2 m above sea level [*Battistini et al.*, 1986]. Just south of the fault, it is 15 ± 2 m above sea level. This implies that this Eemien terrace has been uplifted by 13 ± 2 m by the fault in the last 120 ka. Though detailed modeling of the faulting process [*Feuillet*, 2000] is beyond the scope of this paper, such numbers can be used to crudely constrain the slip rates on the Morne-Piton fault. Taking the footwall uplift over hanging wall downdrop ratios usually measured along normal faults (between 1/2 and 1/3.5) [e.g., *R. Stein et al.*, 1988; *Armijo et al.*, 1996], would imply a slip rate between 0.3 and 0.5 mm/yr on the Morne-Piton fault. Taking the present 1.5–2 m elevation of the wave-cut notch and ledge at the base of the cliff on Figure 9d to result from fault uplift during the Holocene, would imply an average footwall uplift rate of ~0.15–0.2 mm/yr, and a slip rate on the order of 0.7 ± 0.2 mm/yr in the last 10 ka.

3.1.5. Basse-Terre

[19] The volcanic island of Basse-Terre (western Guadeloupe) is composed of five main eruptive complexes emplaced at different times in the last 3.5 Ma (Figure 10) along an overall NNW trend [*De Reynal de Saint Michel*, 1966; *Mervoyer*, 1974; *Westercamp and Tazieff*, 1980; *Dagain*, 1981; *Blanc*, 1983; *Gadalia and Westercamp*, 1984; *Boudon*, 1987]. The youngest volcanic complex (''La Grande Découverte'' recent volcanic complex) formed ~200 ka ago in the southernmost part of the island, between the Monts Caraïbes and the ''axial chain.'' About 560 years ago [e.g., *Boudon et al.*, 1989], the Soufrière dome formed in the middle of this zone, and is still currently active.

[20] The multiepoch volcanic construction of Basse-Terre and the fact that the highest reliefs are sites of

Figure 6. (opposite) (a) Topographic and structural map of La Désirade with fault identification, topography and symbols as in Figure 3a. Small box locates Figure 6b. Lower hemisphere equal area projection of fault planes measured in a Quarry near ''Les Galets'' is shown. Double arrows: inferred local direction of extension (see Figure 6b). Small dots give elevations. Dotted lines offshore: fringing reefs. (b) Detailed mapping of Pointe Des Colibris crack network. Crack strikes are indicated. Dots, sandy areas. Gray, depressions. Full, double arrows indicate local direction of extension inferred from crack strike distribution. Polar diagram of percentages of cracks with a given strike is shown. Inset - Southward aerial view of crack network at Pointe Des Colibris (location in Figure 6a). Black arrows indicate major crack; open black circle, benchmark (5 m elevation). Holocene coral reef is uplifted by about 1 m.

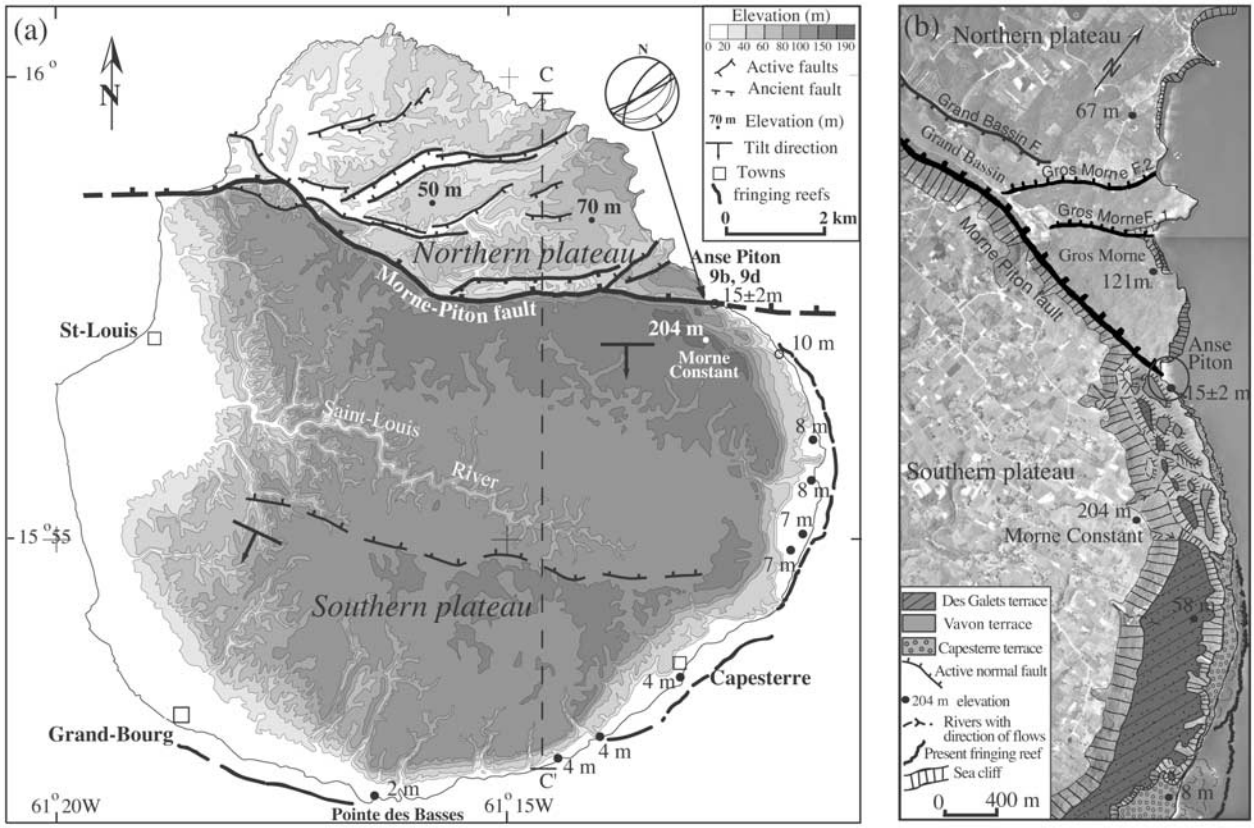

Figure 8. (a) Topographic and structural map of Marie-Galante with fault identification, topography and symbols as in Figure 3a. Ancient fault scarp is dotted black line with ticks. Small black dots: benchmarks. South of Morne-Piton fault, benchmarks are located on the ''Capesterre'' reef terrace and indicate its elevation. Open dots at Anse Piton and 2 km farther south: ''Capesterre'' terrace elevation estimated on the photograph Figure 9d and on topographic map (1/25 000 scale, ING) respectively. Black lines offshore: fringing reefs. Open squares: town locations. Stereoplot shows fault planes and striation measured at Anse Piton. (b) Geomorphic interpretation of Marie-Galante northeastern coast. South of Morne-Piton fault, two principal coral reef terraces are identified, based on analysis of 1/20 000 scale aerial photographs (ING) and 1/25 000 scale topography (ING). Black dots give terrace elevation. Gullies are dashed black lines with flow directions indicated by arrows. Fringing reefs in black. Sea cliff, terraces and Morne-Piton scarp are underlined with thin parallel black lines. Circle: location of Anse-piton (Figures 9b and 9d).

heavy daily rainfall, hence of intense weathering and vegetation growth, make the morphology of the island quite complex. Nevertheless, the southern half of Basse-Terre is cut by large escarpments transverse to the overall trend of the island (Figures 10 and 11). South of Bouillante, on the Caribbean side, two imbricated, horseshoe-shaped escarpments face southward, truncating the axial chain volcanic complex. They have been interpreted to result from two major volcanic collapse sectors and to represent the rim escarpments of the two calderas of Beaugendre and Vieux-Habitants [e.g., *Boudon*, 1987]. Northwest of the Beaugendre ''caldera'' escarpment, a NW striking, fairly continuous step offsets the topography, cutting through high relief almost perpendicular to drainage. South of Piton de Bouillante, there is clear down-to-the-south throw of the upstream part of a NNE flowing catchment along that step, indicative of normal faulting. This fault, which follows part of the ''Marie-Galante-Montserrat'' fault of *Bouysse et al.* [1988] and *Bouysse and Westercamp* [1990], separates the Axial Complex from the Bouillante-Sans-Toucher chain, whose age is constrained between 777 ± 14 and 863 ± 50 ka in this part of the island by K/Ar dating [*Carlut et al.*, 2000]. Toward the east, the fault scarp merges with the Beaugendre and Vieux-Habitants-Matéliane horseshoe-shaped escarpments. Toward the west, after stepping southward, it cuts the coast, and is beautifully exposed in section at Pointe à Sel (Figures 12c and 12d).

[21] South of the Vieux Habitants escarpment, another linear, ≈E-W striking, south facing, topographic scarp cuts the Sans Toucher volcano, and follows to the east the Matéliane ridge and the Sainte Marie river. It does not extend westward directly across the curved Vieux Habitants scarp however. Its length (∼20 km) and linearity attest that it marks a south dipping normal fault that postdates the Sans Toucher volcano, whose age is probably ∼0.8–0.6 Ma.

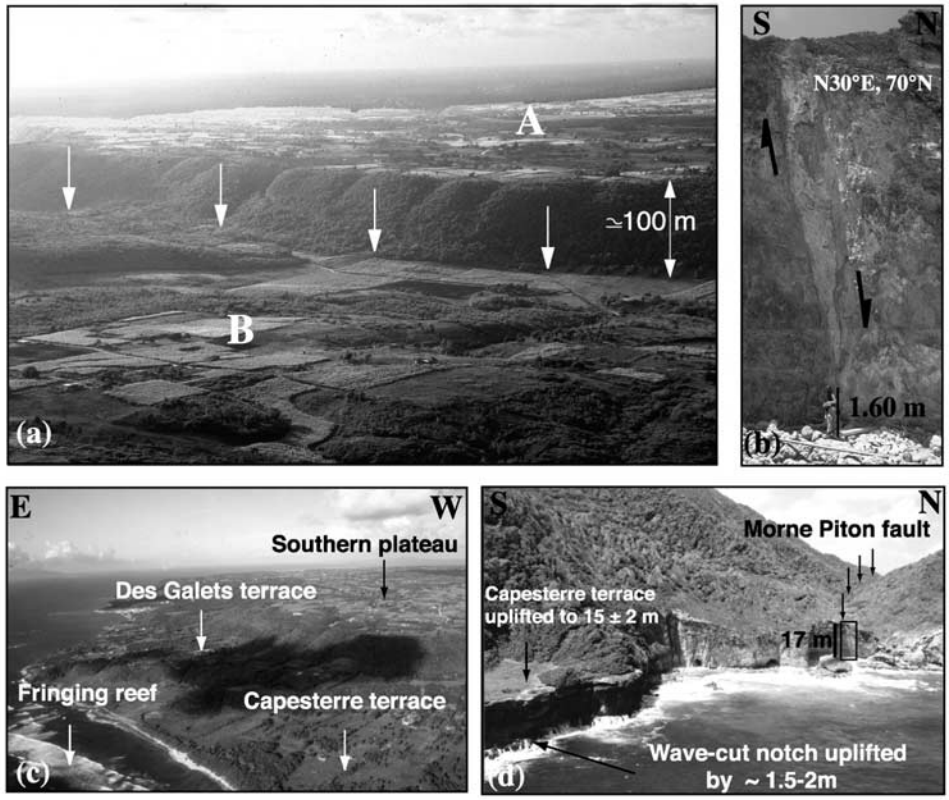

Figure 9. (a) Southeastward view of Morne-Piton fault escarpment. White arrows indicate scarp base. Total cumulative throw is indicated in white. The scarp forms clear, ~100-m-high step in the landscape; northern plateau (B) subsides relative to southern plateau (A) (from *Feuillet et al.* [2001], reprinted from *Comptes rendus de l'Académie des Sciences, Serie II, Sciences de la Terre et des Planètes*, with permission from Elsevier Science). (b) Westward view of major fault plane cutting Anse-Piton cliff to the top (location in Figure 8b). Strike and dip are indicated. Half black arrows indicate slip along fault plane. Scale is given by person. (c) Southward aerial view of inward terrace steps along eastern coast of Marie-Galante southern plateau. Terraces and fringing reef are indicated by arrows. (d) Westward view of uplifted Capesterre terrace and wave-cut notch at Anse-Piton, due south of Morne Piton fault. Small black arrows underline Morne Piton fault trace. Elevations are estimated from scale in background (black line). Location of Figure 9b is indicated.

[22] Northeast of Mateliane, another steep, NW trending, south facing tectonic scarp cuts the northeast flank of the Axial Chain volcanic complex [e.g., *Grellet et al.*, 1988], offsetting at high-angle crests and intervening river channels.

[23] More recent volcanic edifices and deposits, with younger forms and smoother surfaces, extend south of the Mateliane-Sans Toucher escarpment. The two most prominent eruptive centers are the Carmichaël and Icaques volcanoes. The northern flank of Carmichaël is mantled by flows and pyroclastic deposits that diverge away from the Caribbean-Atlantic water divide (Figures 10 and 11a). The Icaques volcano shows a conspicuous half crater. Both edifices are truncated and limited by south facing scarps (Crète des Icaques, Montagne de Capesterre and Grande-Découverte). The Icaques volcano is ~600 ka old, within the 1.2–0.6 Ma age span of volcanic rocks in the Bouillante chain [*Blanc*, 1983]. The Carmichaël volcanics are 140–11.5 ka old [*Blanc*, 1983; *Boudon et al.*, 1990; *Carlut et al.*, 2000] and may have formed within another horseshoe collapse sector [*Boudon et al.*, 1992] truncating the Icaque volcano (Figures 11a and 11b, cross section b).

[24] Finally, the northern boundary of the most recent part of the "Carmichaël-Soufrière complex" follows the base of the Grande-Découverte scarp and the Baillif river.

[25] Hence, all in all, the major topographic escarpments that limit the different imbricated volcanic edifices southeast of Bouillante have similar trends (N50°E to N90° ± 10°E) and follow south dipping normal faults.

[26] Southeast of the Soufrière dome and of the Echelle and Citerne scoria cones, a series of 11–17 ka old [*Dagain*, 1981] andesitic vents (Morne Lenglet, Gros Fougas, Madeleine, Morne Liquin) [e.g., *Boudon et al.*, 1990] are aligned along an ~E-W trend, due west of an E-W striking, 30-m-high, offshore normal fault scarp (Figure 11a). These andesitic vents thus probably formed recently along a fissure marking the westward continuation of the offshore normal fault.

[27] The recent volcanics are limited to the south by the Monts Caraïbes complex, whose lavas were mostly emplaced ~500–400 ka ago [*Blanc*, 1983], in part coevally with those of the Bouillante chain. Roughly E-W trending, north dipping normal faults bound the Monts Caraïbes to

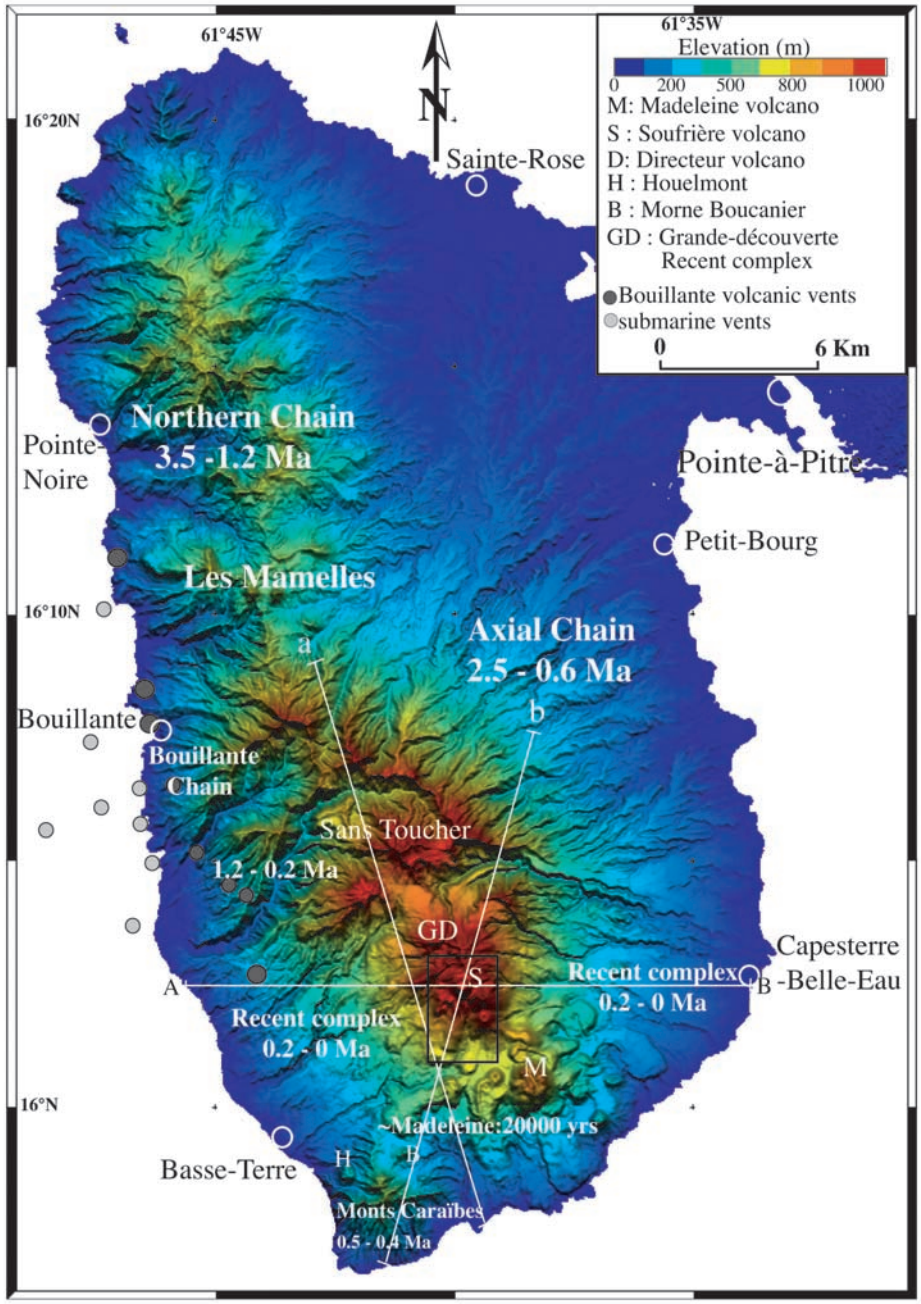

Figure 10. Digital Elevation Model of Basse-Terre (from IGN), illuminated from NNW. Horizontal resolution: 50 m. GD, Grande-Découverte; S, Soufrière; M, Madeleine; H, Houëlmont, B: Morne Boucanier. Ages of main volcanic complexes are indicated. Open white circles: localities. White lines a, b: geological cross sections of Figure 11b; AB: topographic profile of Figure 15b. Box: location of Figure 12a.

Figure 11a. (opposite) Geological, morphological and structural map of southern Basse-Terre. Ages (white boxes) are from *Blanc* [1983] and *Carlut et al.* [2000]. Bathymetric contours from SHOM (1/60 000 scale, 1987) with depth indicated in gray, blue. Faults and symbols as in Figure 3a. Geology and morphology, north and south of Grande-Découverte-Carmichaël complex, are based on analysis of DEM, aerial photographs (1/20000 scale), topographic maps (1/25000 scale), and previous work [e.g., *De Reynal de Saint-Michel*, 1966; *Blanc*, 1983; *Gadalia and Westercamp*, 1984; *Carlut et al.*, 2000]. Contours of 11500 and 3100 B.P. debris flows, and of 30-17-kyr pumice and lava flows are from *Boudon et al.* [1989]. Grande-Découverte-Carmichaël complex and Madeleine-Trois Rivières eruptive center domes and lava flows (orange-red and pale yellow, respectively) are mapped from *Boudon* [1987] and *Boudon et al.* [1990], slightly modified based on our DEM geomorphic interpretation. GDF, Grande-Découverte fault; black open circles, towns; rivers, in dashed blue lines; crests, in thin black lines; morphological escarpments underlined by parallel thin black lines. Arrows indicate lava flow directions. White dots indicate peaks, with elevation indicated. Lava flows edges are underlined by black dashed lines. See discussion in text.

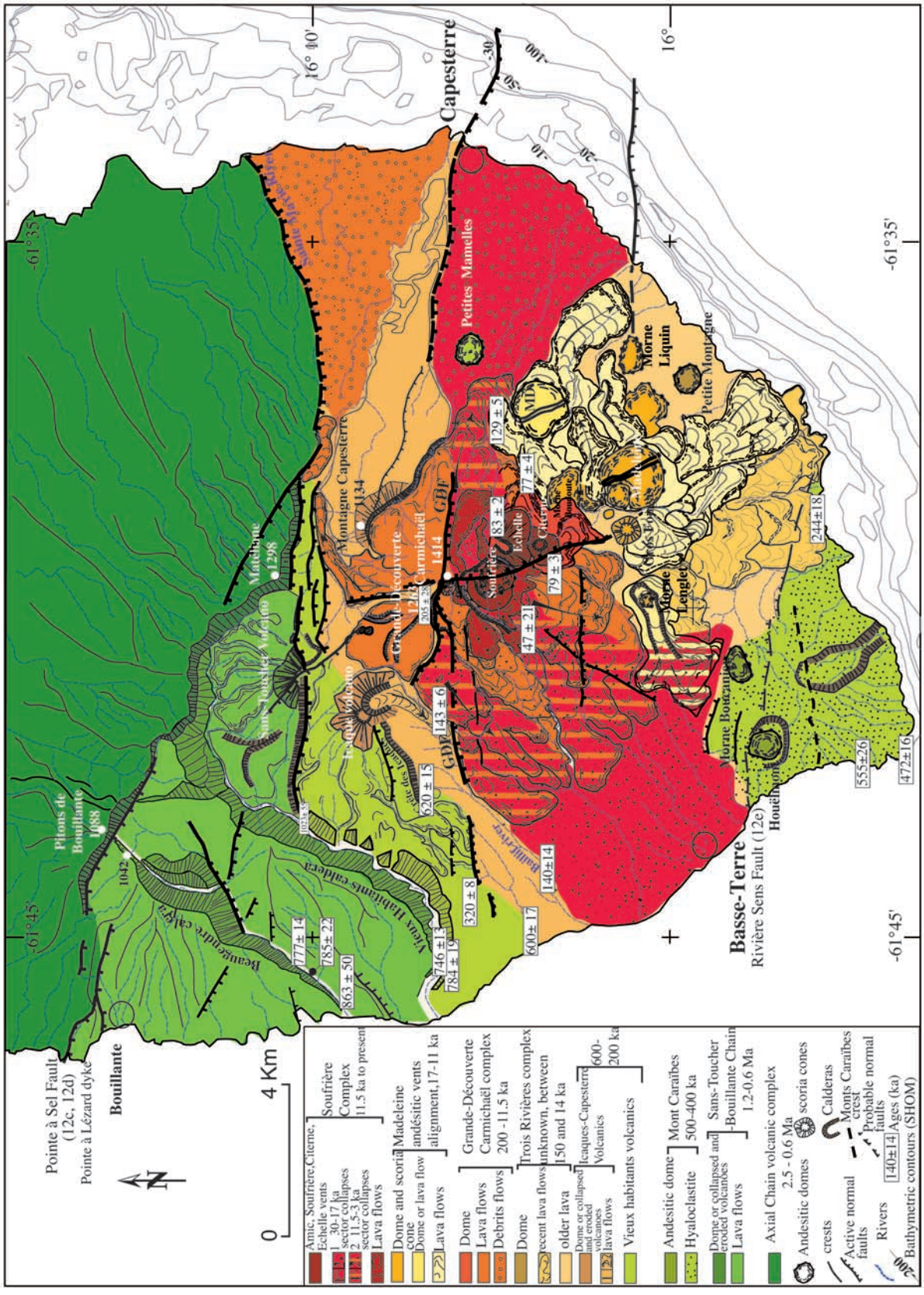
Pointe à Sel Fault
(12c, 12d)
Pointe à Lézard dyke
Bouillante
Pitons de Bouillante
1088
1042
Beausoleil caldera
Vieux Habitants caldera
Madeleine
1298
Montagne Capesterre
1134
Grand Découverte
1205
Carmichaël
1414
GBF
Capesterre
Petites Mamelles
Morne Liquin
Petite Montagne
Morne Bouganier
Morne Lengle
Basse-Terre
Rivière Sens Fault (12e)
Houëlmont
Bouillante Fault
-61°45'
-61°35'
16° 40'
16°
0
4 Km
N
Amic, Soufrière,Citerne,
Echelle vents
1 30-17 ka
sector collapses
2 11.5-3 ka
sector collapses
Lava flows
Soufrière Complex
11.5 ka to present
Dome and scoria cone
Dome or lava flow
Madeleine andésitic vents
alignment,17-11 ka
Lava flows
Dome
Lava flows
Debrits flows
Grande-Découverte Carmichaël complex
200 -11.5 ka
Dome
recent lava flows
Trois Rivières complex
unknown, between
150 and 14 ka
older lava
Dome or collapsed and eroded volcanoes
lava flows
Icaques-Capesterre Volcanics
600-200 ka
Vieux habitants volcanics
Andesitic dome
Hyaloclastite
Mont Caraïbes
500-400 ka
Dome or collapsed and eroded volcanoes
Lava flows
Sans-Toucher Bouillante Chain
1.2-0.6 Ma
Axial Chain volcanic complex
2.5 - 0.6 Ma
Andesitic domes
scoria cones
crests
Calderas
Monts Caraïbes crest
Active normal faults
Probable normal faults
Rivers
140±14 Ages (ka)
Bathymetric contours (SHOM)

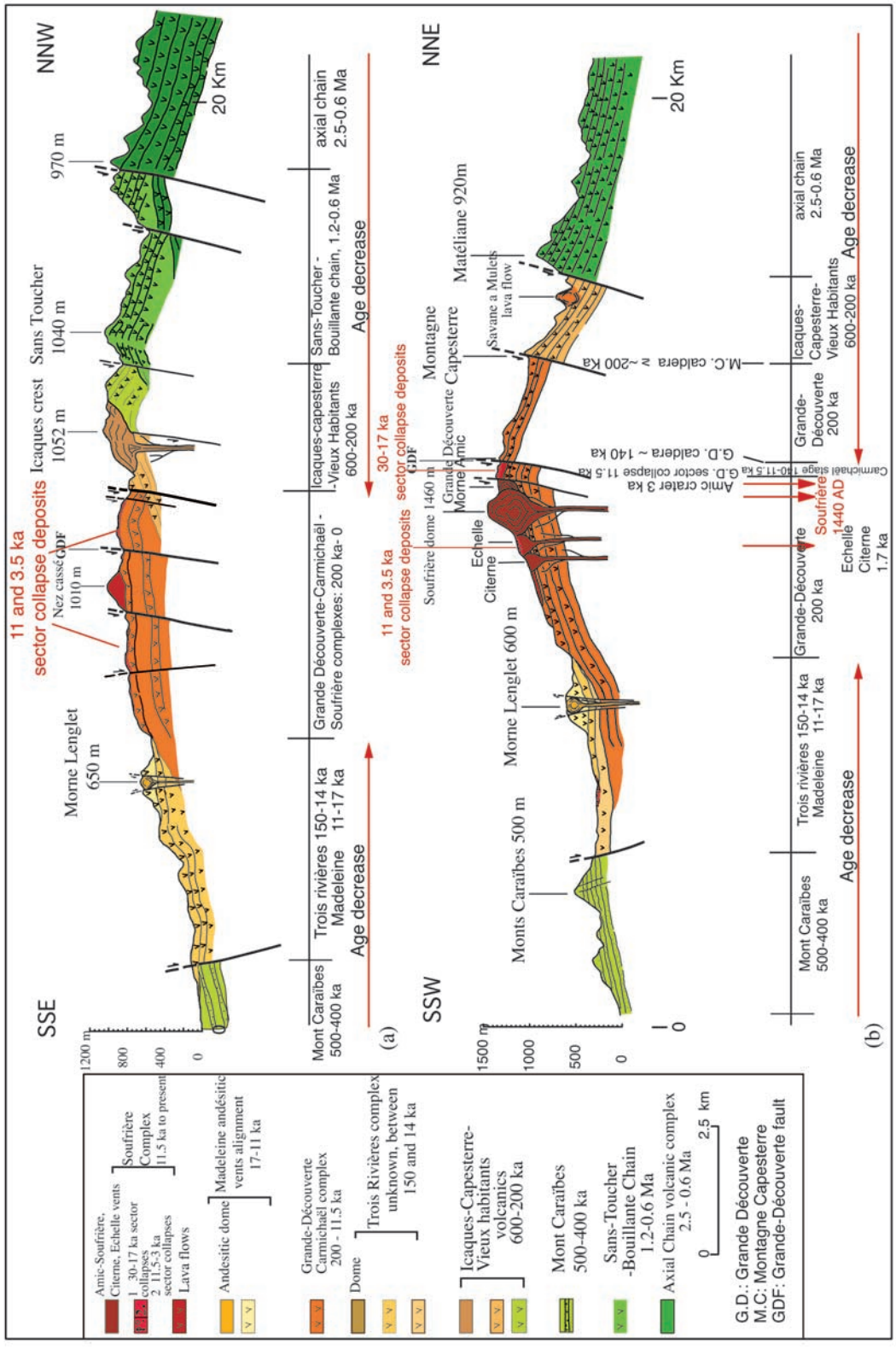

Figure 11b. Geological sections across southern Basse-Terre (location in Figure 10), based on geological, morphological, and structural interpretation of Figure 11a. GDF, Grande-Découverte fault. Horizontal red arrows indicate overall volcanic complex age decrease. Vertical exaggeration: 2. The youngest volcanic vents (Soufrière and Madeleine) are between two antithetic normal fault sets; see discussion in text.

the north. In the east, such faults are unconformably overlain by the late Pleistocene andesitic flows of the Madeleine vent alignment.

[28] In summary, the overall morphology and the ages and emplacement pattern of the volcanics suggest that southern Basse-Terre is cut by two antithetic normal fault sets facing each other on either side of the recent volcanic complex (Figure 11). This complex thus fills a roughly E-W trending, graben-like trough between more ancient volcanic rocks to the north and south. The Madeleine andesitic vents likely reflect late Pleistocene fissuring parallel to the axis of that graben.

[29] Concurrently however, north of those vents, there is another, ''en echelon,'' NNW trending alignment of volcanic cones that follows roughly the water divide. This direction, parallel to that of the Caribbean volcanic arc, also coincides with the direction of the fissures that cut the Madeleine and the Morne Dongo domes, and the surface trace of the Ty normal fault across the summit of the Soufrière dome and the western flank of the Citerne scoria cone (Figures 11a and 12a). The fresh scarp of this active fault, which strikes ~N0 to N160°E, at high angle to the boundary faults of the graben, dips steeply eastward, and is ~6 km long and at most ~5 m high (Figures 12a and 12b). To the north, the Ty fault cuts the Grande Découverte escarpment and extends across the Grande Découverte-Carmichaël complex along two smaller, left stepping, east dipping segments. Farther north, it may continue along the 3-km-long, NW striking, west dipping, normal fault scarp that offsets the E-W striking Matéliane-Sans Toucher escarpment and the Sans-Toucher volcano.

[30] To better constrain the Quaternary fault geometry and kinematics in Basse Terre, we studied in detail the western coast of the island, where outcrops are well exposed. We measured many fault planes, a few of them bearing slickensides. All measurements are reported in Figure 13.

[31] Clear fault planes are observed between Anse Colas and Pointe à Sel, cutting the 2.5–0.6 My-old volcanic rocks north of Bouillante (n°1–10, Figure 13). The faults strike between N60° and N120°E, with an average direction of N100°E. More than two thirds of them dip southward. The main faults were observed at Falaise Bellon, Pointe à Sel and Anse à Sable (10, 9, 6, Figure 13). At Pointe à Sel (n°10, Figure 13), a large, E-W striking, 75°S dipping normal fault offsets the Bouillante volcanic deposits by at least 30 m, juxtaposing a thick pumice flow with coarse pyroclastic deposits (Figures 12c and 12d). The fault breccia is ~1 m thick. The fault footwall is cut by synthetic, secondary N96°E striking normal faults. Near Malendure beach, The N70°E striking, 70°S dipping plane of one of the largest faults bears slickensides with 55°W pitch, attesting to normal, dextral slip (n°7, Figure 13). Another fault north of Malendure exhibits slickensides with 86° NW pitch on a ~N110°E striking, 75°N dipping plane (n°3, Figure 13), implying a sinistral slip component. The overall fault kinematics is therefore consistent with an extension direction slightly east of north.

[32] South of Bouillante, between Pointe du Quesy and Anse du Val de l'Orge, i.e., in the recent volcanic complex, we observed a great number of open fissures, many reaching the ground surface. The largest strike N80° ± 20°E and are several tens of centimeters to ~1.5 m wide. There were also a few small N105° ± 5°E striking normal faults with throws of several centimeters (n°11–16, Figure 13).

[33] The volcanic complex of the Monts Caraïbes is cut by N20° to N100°E striking normal faults with throws up to several meters. Seventy percent of these faults dip northward (n°17–21, Figure 13). All cut unconsolidated hyaloclastites that are more basaltic in composition than rocks to the north (Figure 12e).

[34] To summarize, our morphotectonic and microtectonic study reveals that the southern part of Basse-Terre is cut by Quaternary normal faults, most of them striking ~E-W. Most of the faults north of the recent volcanics dip southward. This is where the largest offsets are found. South of Pointe du Quesy, mostly open fissures are observed. Their directions are more variable, and include N20°–60°E planes. There are no visible ''tectonic feature'' between Anse du Val de l'Orge and Rivière de Sens, in the most recent (<11 ka) debris flows, where the coastline shows no steep cliff. Faults in the Mont Caraïbes complex strike between ~E-W and N20°E, and on average N60°–70°E. Most of them dip northward, implying that the Mont Caraïbes were uplifted relative to the recent volcanic complex, a situation antithetic to that observed on the north side of this complex.

3.1.6. Synthesis

[35] Overall, all the islands of the Guadeloupe archipelago are thus cut by predominantly Quaternary normal faults, whose lengths vary from a few tens of meters to more than 10 km, with throws from a few centimeters to more than 100 m. The morphology of the fault scarps, and the fact that most are associated with arrays of parallel, open fissures reaching the surface, imply that the faults are active and accommodate current extensional strain. Most of the faults, with the exception of those in the north of Grande Terre, strike on average N60° to N140°E. South of ~16°20′N, the dominant fault population is even more homogeneous, with a mean strike around N70°–100°N. Most faults show either en echelon segmentation or striated planes that testify to oblique slip, either normal-right-lateral on planes striking ~N70°–100°E, or normal-left- lateral on planes striking N110°–140°E. This is consistent with roughly N-S extension, nearly parallel to the arc. A ~N0° ± 10°E direction of extension would account for most kinematic observations, again with the exception of the faults in the northern part of Grande-Terre (~N110°E extension), and of one system of faults and fissures in the southern part of Basse-Terre, in the active volcanic complex (Ty fault, ~N75° ± 5°E extension).

3.2. Faulting at Sea

[36] The bathymetric chart in Figure 14a, redrawn from those compiled by *Bouysse et al.* [1984], is based on the bathymetric and Seabeam data acquired during the ARCANTE cruises [*Bouysse et al.*, 1983a; *Polyak et al.*, 1992] and on the echo-sounding data acquired by the French Hydrographic Service.

[37] Linear perturbations in bathymetric gradients delineate submarine fault scarps with normal throw [e.g., *Manighetti et al.*, 1997], that offset the seafloor around the

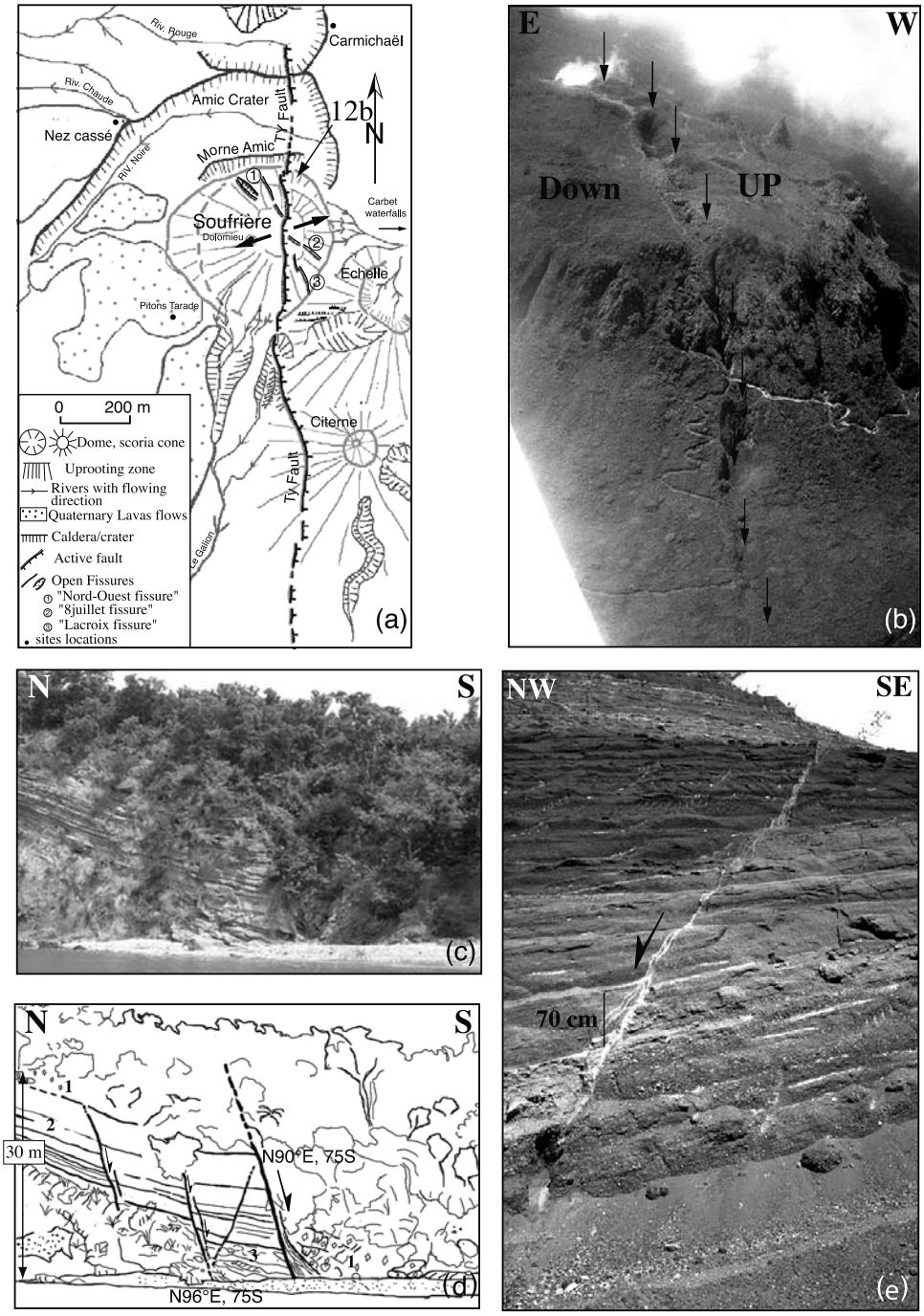

Figure 12. (a) Morphological and structural map of the Soufrière massif. Faults as in Figure 3a. Black arrow: location of Figure 12b; double black arrows: local extension direction deduced from fault and fissure strike distribution. (b) Southwestward view of Ty fault scarp, about 5 m high, underlined by black arrows. Up: uplifting footwall; Down: downdropping hanging wall. (c and d) Westward view of Pointe à Sel normal faults, and tectonic interpretation. 1, coarse debris flow deposits; 2, pumice flow; 3, pyroclastic flow. Half arrows: Hanging wall slip. Fault plane measurements are given. Fault breccia, at major fault base, in thin lines. Double arrows: cliff elevation (from *Feuillet et al.* [2001], reprinted from *Comptes rendus de l'Académie des Sciences, Serie II, Sciences de la Terre et des Planètes*, with permission from Elsevier Science). (e) Northeastward view of a N65°E striking, north dipping normal fault, with ∼1 m of throw, offsetting the Monts Caraïbes hyaloclastites, up to surface, in quarry. Note that, in section, the fault plane is associated with en echelon, open fissures compatible with normal slip (from *Feuillet et al.* [2001], reprinted from *Comptes rendus de l'Académie des Sciences, Serie II, Sciences de la Terre et des Planètes*, with permission from Elsevier Science).

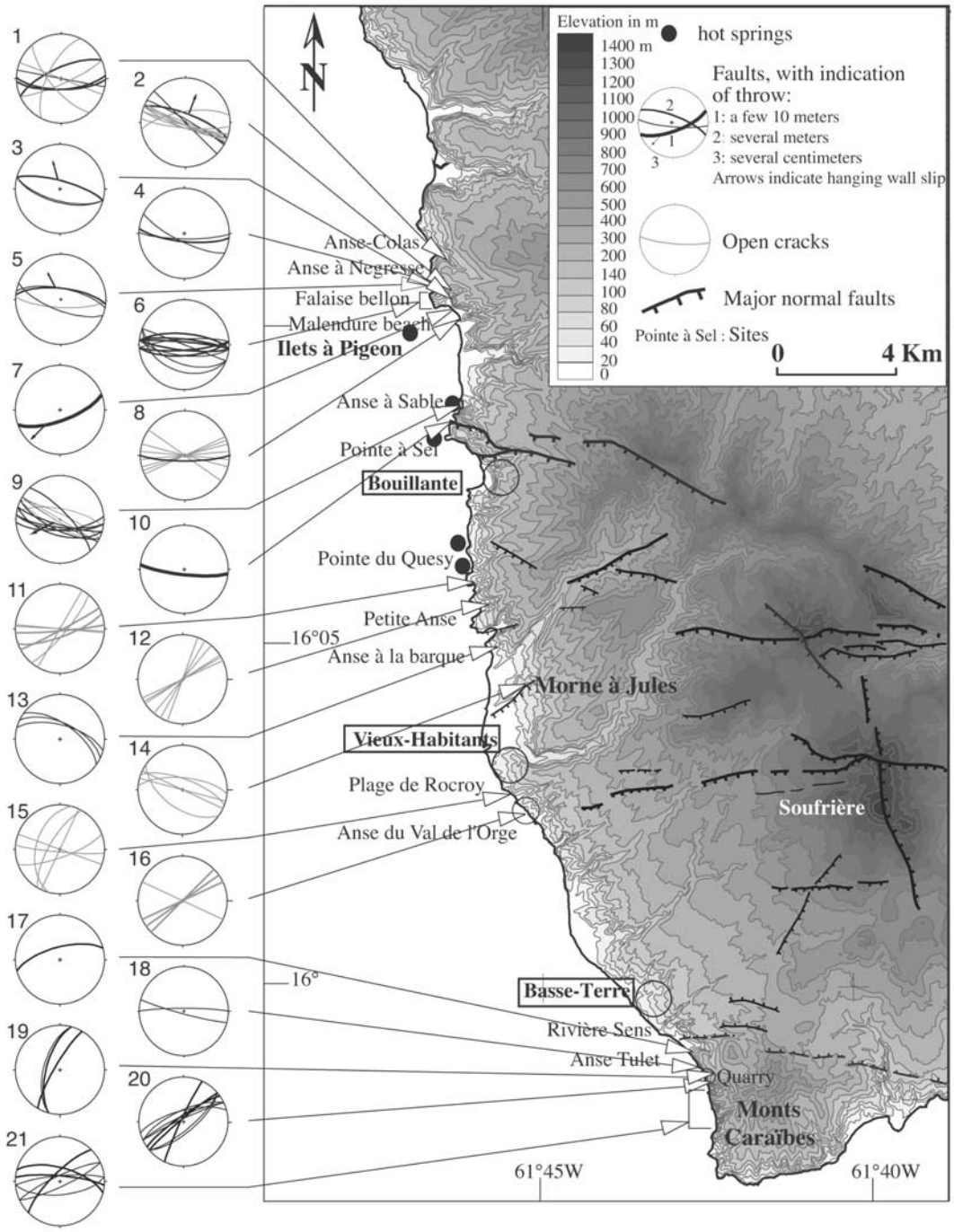

Figure 13. Tectonic and microtectonic observations and measurements in southern Basse-Terre. Topography redrawn from topographic maps (1/25 000, IGN); faults as in Figure 11a. White arrows point to different measurement sites. Stereoplots 1–21 are lower hemisphere equal area projections of measured faults (black) and cracks (gray) planes and associated striations (arrows: hanging wall slip). Thicker planes for major faults and fissures. Open black circles are localities. Note that hot springs (black dots) are localized along the coast, north and south of Pointe à Sel fault (from *Feuillet et al.* [2001], reprinted from *Comptes rendus de l'Académie des Sciences, Serie II, Sciences de la Terre et des Planètes*, with permission from Elsevier Science).

islands. Figure 14a shows the principal faults we mapped. Two deep, elongated fault-bounded troughs appear to dissect the eastern, coral-capped shelf of the Guadeloupe archipelago. The deepest one, the ''Désirade valley,'' extends north of La Désirade and northeast of Grande Terre. The shallower one, the ''Marie-Galante valley,'' separates Grande Terre and La Désirade from Marie-Galante and Les Saintes.

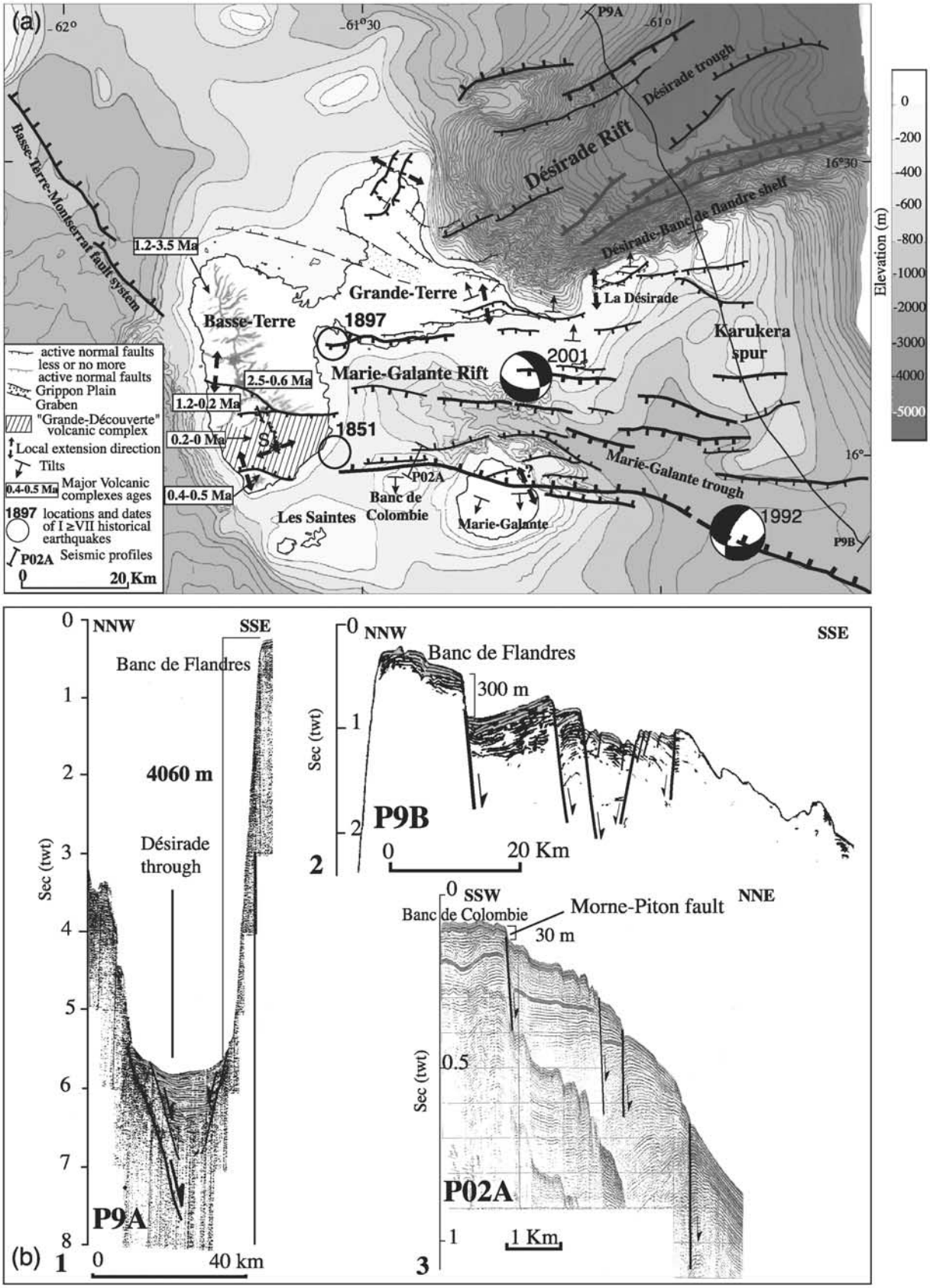
(a)
-62°
-61°30
-61°
P9A
Désirade trough
Désirade Rift
16°30
Basse-Terre-Montserrat fault system
1.2-3.5 Ma
Désirade-Banc de flandre shelf
Grande-Terre
La Désirade
Basse-Terre
1897
2001
Karukera spur
Marie-Galante Rift
2.5-0.6 Ma
1.2-0.2 Ma
0.2-0 Ma
1851
0.4-0.5 Ma
P02A
Banc de Colombie
Les Saintes
Marie-Galante
Marie-Galante trough
16°
1992
P9B
active normal faults
less or no more active normal faults
Grippon Plain Graben
"Grande-Découverte" volcanic complex
Local extension direction
Tilts
Major Volcanic complexes ages
locations and dates of I ≥VII historical earthquakes
Seismic profiles
0 20 Km
Elevation (m)
0
-200
-400
-600
-800
-1000
-2000
-3000
-4000
-5000
(b)
NNW
SSE
Banc de Flandres
4060 m
Désirade through
Sec (twt)
P9A
1
0 40 km
2
300 m
P9B
0 20 Km
SSW
NNE
Banc de Colombie
Morne-Piton fault
30 m
0.5
P02A
1 Km
3

[38] The Désirade trough is a WSW striking depression, more than 80 km long, ~30 km wide and up to 5500 m deep. The inner floor of this trough is bounded by antithetic normal faults. The southern, ≈N70° striking wall of the trough forms a steep submarine escarpment ~4000 m high. The northern wall is broader, smoother and more gently sloping. The Désirade graben is therefore asymmetric. If the floor of the trough were made of rocks similar to those observed beneath the reef limestones that cap La Désirade and perhaps the Banc de Flandre, the cumulative vertical throw along the southern wall of the Désirade trough might exceed 4000 m. A seismic reflexion profile across it yields insight into its structure [*Bouysse et al.*, 1983a] (P9A, Figure 14b). To the north, sediments pond against two synthetic normal faults. The steepness of the southern wall prevents identification of possibly different, parallel, normal faults. The graben is filled with ≈2000 m of sediments, implying a cumulative throw on the southern fault system of ~6000 m. The south dipping normal faults that bound the north side of the graben appear to encroach upon the northeastern coast of Grande Terre, after veering toward a more southwesterly direction (Figure 14a). The onland terminations of these faults thus probably correspond to the Grande-Vigie, Montagne Vercinot and Grippon faults. The depth of the Désirade trough's inner floor shallows westward, as its width narrows, giving the graben a west pointing V-shape in map view. The cumulative vertical throws of the faults decrease from east to west as the faults terminate onland in Grande Terre. All this suggests that the Désirade graben faults might have propagated westward [e.g., *Manighetti et al.*, 1997]. Surprisingly, however, the southern, north facing escarpment of the Désirade graben, which has the greatest cumulative throw, stops short of the eastern coast of Grande-Terre, which suggests that the corresponding faults, although arguably the largest in the archipelago, may not be active anymore.

[39] The aligned reef plateaus of Grande Terre, La Désirade, and Banc de Flandre are separated from the Banc de Colombie and Marie-Galante reef tables by the WNW-ESE striking "Marie-Galante graben," which is over 120 km long and at most 1500 m deep. This graben's floor is flanked by two active, antithetic normal fault systems. The outer faults of those systems cut the reefs onland while the inner faults are visible both in the bathymetry and on seismic sections P9B and P02A roughly perpendicular to the graben [*Bouysse and Guennoc*, 1983; *Got et al.*, 1985; *Inoubli*, 1981] (Figure 14b).

[40] The southern, northward dipping fault system is narrower and less segmented than the northern one. The main, ≈E to ESE striking, normal fault is over 100 km long and crosses Marie-Galante along the base of the Morne-Piton scarp. This Morne-Piton fault is particularly clear on seismic profile P02A (Figure 14b). Its throw reaches up to ≈100–200 m in the east, but decreases westward as the fault splays into parallel, synthetic faults. The submarine Morne-Piton fault scarp is little more than 30 m high where it bounds the Banc de Colombie. As the southern plateau of Marie-Galante, the Banc de Colombie is tilted southward by the Morne-Piton fault, by ~0.8°. At this scale, right stepping jog of the fault across the island may indicate a right-lateral component of slip on the longer ~E-W stretches of the fault.

[41] The fault system bounding the Marie-Galante trough to the north is broader than the southern one, though it narrows from ≈40 to 10 km from east to west. It is made of shorter (≈20 km long), south dipping normal faults, the mean strike of which varies from ≈N100° to N80°E from south to north. The northernmost faults, which cut and bound to the south the Banc de Flandre, appear to be the continuation of the faults identified along the southern shore of La Désirade and Grande Terre. Some of them are observed in cross section along seismic profile P9B (Figure 14b). They offset the seafloor along steep scarps, several tens of meters high on average, with a maximum height of ≈300 m for the faults bounding the southern edge of Banc de Flandre. Motion on most of them has tilted northward the footwall blocks they bound (e.g., La Désirade, Petite-Terre), contributing to shape them in elongated, ENE to E-W strips. Overall, the Marie-Galante trough is an asymmetric graben with greater throw on the south dipping faults, at least to the east. Such asymmetry is also observed for the faults that cut the Soufrière volcanic complex. As for the Désirade trough, the depth of the Marie-Galante inner floor shallows westward, while its width narrows and both the number and throw of the faults that bound it decrease from east to west. This suggests that the Marie-Galante graben has also propagated westward.

[42] Northwest of Basse-Terre, the seafloor is cut by the ~N150°E striking Basse-Terre-Montserrat normal fault system [*Got et al.*, 1985; *Polyak et al.*, 1992] which we interpret to mark the offshore continuation of the Ty fault. This system appears to be composed of right stepping segments accommodating a left-lateral component of slip along the volcanic arc [*Feuillet*, 2000]. The Marie-Galante and Désirade graben faults connect westward with the Basse-Terre-Montserrat faults, implying they are coeval.

3.3. Synthesis

[43] Consistent evidences both onland and underwater support the inference that the Guadeloupe archipelago is dissected by two normal fault-bounded grabens, striking

Figure 14. (opposite) (a) Bathymetric and tectonic map of Guadeloupe archipelago. Bathymetry is redrawn from *Bouysse et al.* [1983a, 1984] and *Polyak et al.* [1992]. Onland, faults are from Figures 3a, 6a, 8a, and 11a; underwater, from interpretation of bathymetric contour patterns and seismic profiles; see discussion in text. Hatched area: recent volcanism (<0.2 Ma); S, Soufrière. Double black arrows indicate local extension direction estimated from microtectonic measurements and fault geometry. Thin black lines are seismic profiles. Ages (in Ma) in boxes are from Figures 10 and 11a. Earthquakes focal mechanisms from Harvard catalog, see caption of Figure 2. Locations and dates of $I \geq$ VII, shallow, historical earthquakes are indicated (black open circles) from *Feuillard* [1985] and *Bernard and Lambert* [1988]. See discussion in text. (b) Seismic reflexion profiles across Guadeloupe archipelago [from *Bouysse*, 1979; *Bouysse et al.*, 1983a; *Got et al.*, 1985; *Inoubli*, 1981] (location in Figure 14a). Faults are in black lines, with hanging wall slip indicated by arrow. Major fault scarp heights are indicated. 1- Profile P9A across Désirade trough; 2- Profile P9B across Karukera spur; 3- Profile P02A across Colombie Bank.

roughly perpendicular to the trench. The Désirade trough is ≈3–4 times deeper and wider than the Marie Galante graben. There is little evidence of active, ongoing slip along its southern, largest bounding fault, however. We therefore infer that it is older. In fact, it is likely that it started to form prior to 2 My ago, unless downthrow rates exceeded those observed along most rift bounding faults (≤3 mm/yr) [e.g, *Stein et al.*, 1991; *Manighetti et al.*, 1998]. Both rifts seem to have propagated westward with both of their tips encroaching upon the main islands of Guadeloupe. The two facing normal fault systems identified on either side of the recent volcanic complex of Basse-Terre mark the western termination onland of the Marie-Galante rift, which is the most recent (probably ∼0.5 Ma old) and most active of the two.

4. Relationship Between Active Tectonics and Volcanism

[44] The recent volcanic complex of Basse-Terre lies entirely within the western termination of the active Marie-Galante rift (Figure 14a). The older Désirade graben terminates westward just east of the older, northern volcanic complex of Basse-Terre. The cumulative vertical throws of the Marie Galante rift bounding faults imply that such faults have been active for a few hundred thousand years at most. The Désirade rift, by contrast, started to form at least a few millions years ago and is less active today. Such ages are roughly synchronous with the main volcanic building epochs that formed the 1.2–3.5 Ma old basement of northern Basse-Terre, and the ∼0.7 Ma old ''recent volcanic complex'' of southern Basse-Terre. Thus there seems to be a relationship, in terms of geometry and timing, between volcanism and rifting in this part of the Caribbean Arc. Both the most ancient and the most recent volcanic complexes seem to have developed at the western tip of rifts that were propagating westward, right at the intersection between such rifts and the deep magma source that follows the volcanic arc.

[45] The location of the active Soufrière volcanic complex at the tip of the active Marie-Galante rift is particularly remarkable. The rift extends between the two antithetic normal fault sets that heave the older volcanic basement of the Monts Caraïbes and axial-Bouillante chains on either side (Figure 15a). It is limited to the north by the large escarpments that follow the Matéliane and Grande Découverte crests, and to the south by the northern boundary of the Monts Caraïbes. The various eruptive products (pyroclastic debris flows, andesitic flows, ash layers, extrusive domes, etc.) of the recent volcanic complex floor the entire area between these escarpments, from coast to coast. To the north and south, the outer walls of the escarpments probably act as topographic buttresses while the volcano slopes extend regularly down beneath the Caribbean sea and Atlantic Ocean to the west and east (Figure 15a). This may account for the predominance of southwest or southeast directed sector collapses and blasts with pyroclastic avalanches in those directions throughout the buildup of La Grande Découverte. In recent times, for instance, large pyroclastic avalanches have been directed toward the Atlantic ∼30 and 17 ka ago, whereas more recent ones (11.5 and 3.1 ka ago) blasted predominantly into the Caribbean sea [*Boudon et al.*, 1984; *Boudon*, 1987; *Boudon et al.*, 1987, 1990, 1992]. The E-W topographic profile across the Soufrière (Nez-cassé, Soufrière, Echelle, Figure 15b) shows that the currently active volcanic massif is asymmetric, with an eastern flank much steeper (25°) than the western one (15°). Such steepness toward the east probably makes the former flank more unstable than the latter. Current down to the east cumulative throw on the ∼N-S striking Ty fault, which is the main fault and fissure system to cross the volcanic dome, and is marked by an east facing scarp over 5 m high, probably reflects this large-scale instability. It is thus possible, if not likely, that the next collapse episode of the volcano summit will occur in an ESE direction, toward Capesterre rather than Saint Claude and Basse-Terre, as the last large blast avalanche did 3100 years ago (Figure 15a).

5. Seismicity and Active Faulting in and Around Guadeloupe

[46] Figure 16 shows the shallow seismicity recorded, between 1981 and 1995, by the two seismic networks maintained in Guadeloupe and Martinique by the Institut de Physique du Globe. Although the elongated geometry of the network introduces a bias in hypocenter location determination, it yields an acceptable first-order view of the overall seismicity distribution. The epicenters plotted in Figures 16 and 2b are from the annual reports of the Observatories of Guadeloupe and Martinique. A calibration shot made east of Martinique shows that epicentral errors are usually <5 km for superficial events occurring within the network, while the depth uncertainties are on order of 7–10 km [*Dorel*, 1981; *Girardin et al.*, 1991]. For the events outside of the network (i.e., north of 17°N or south of 14°5 N), epicentral errors are greater, on order of ∼20 km [*Dorel*, 1981].

[47] We have also reported in Figure 16 the main normal faults defined in this study or inferred from the overall bathymetry (see Figure 17).

[48] Shallow seismicity is especially strong along the Marie-Galante graben. This confirms that the graben bounding faults are active, as inferred from morphology onland. The focal mechanisms of the $mb = 5.6$, August 3, 1992, and $M_s = 4.6$, January 5, 2001, shocks that occurred at a depth of ∼10–15 km within the overriding plate, ∼40 km east and 20 km northeast of Marie-Galante, respectively, are compatible with oblique slip on ∼E-W striking, south dipping planes. These earthquakes may have ruptured the faults that bound the edges of the Marie-Galante trough and the Karukera spur. Many $M_d > 3.5$, shallow shocks also occur in the same area. Two fairly large historical earthquakes, with maximum intensities of VII to VIII, have occurred between Grande-Terre and Marie-Galante in the last 150 years (Figures 2 and 14a) [e.g., *Feuillard*, 1985; *Bernard and Lambert*, 1988]. The epicenter of the shallow, locally destructive 29 April 1897 earthquake ($m \approx 5.5$–6) [*Bernard and Lambert*, 1988] has been located near Pointe à Pitre, close to the western end of the Gosier fault. We infer that it ruptured this fault. That of the 16 May 1851 earthquake, whose magnitude was comparable [*Bernard and Lambert*, 1988], has been located near Capesterre. It may also have ruptured one of the shallow normal faults at the western end of the Marie-Galante graben.

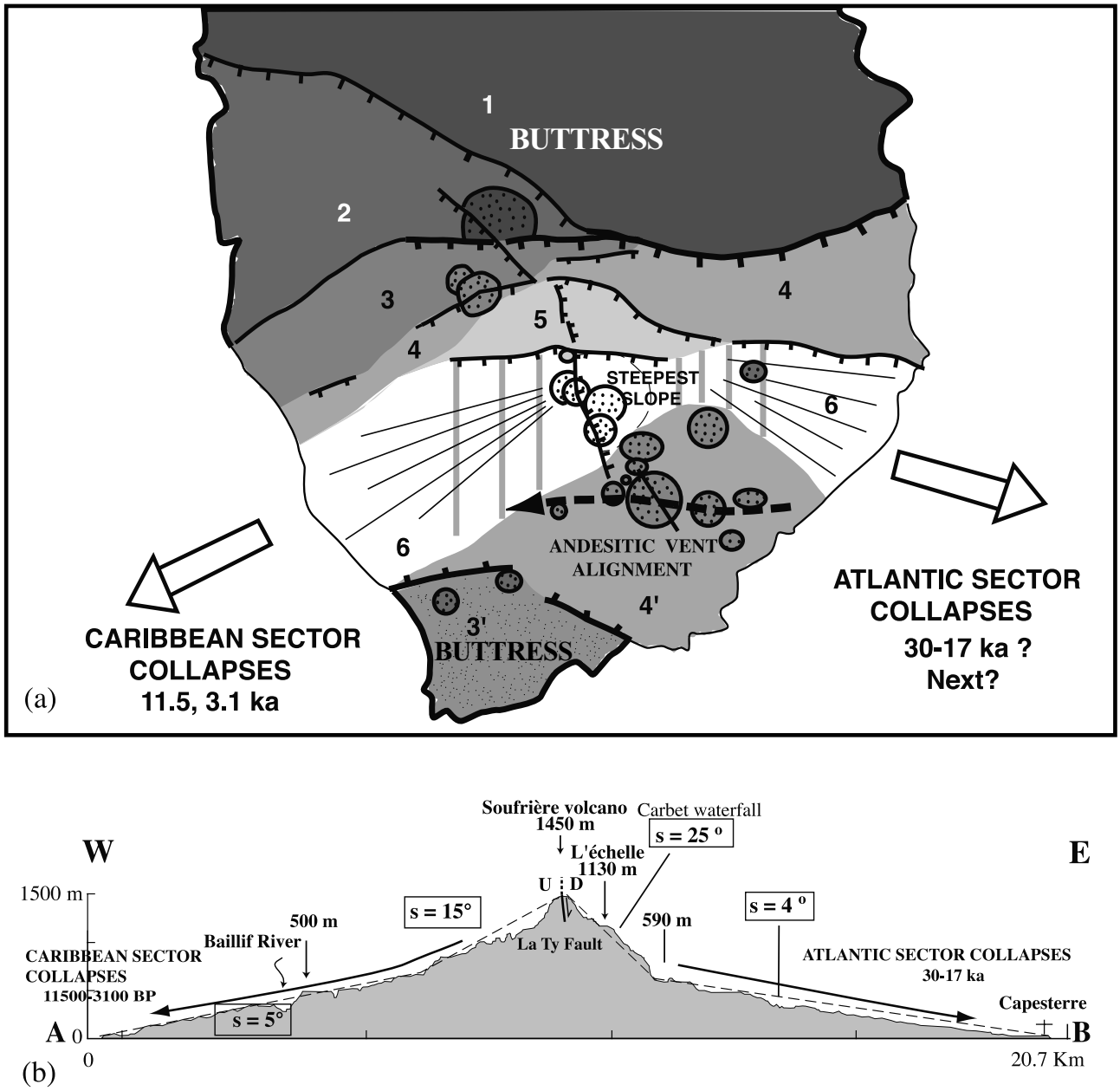

Figure 15. (a) Volcano-tectonic model of southern Basse-Terre. Faults and volcanic zones are simplified from Figure 11a. 1, Axial chain; 2, Bouillante-Sans Toucher complex; 3, Vieux Habitants volcanics; 3′, Monts Caraïbes; 4, Icaques-Capesterre volcanics; 4′, Trois-Rivière-Madeleine complex; 5, Grande-Découverte-Carmichäel; 6, Soufrière complex. Circles filled with dots: scoria vents and andesitic domes. Dashed black arrow, inferred westward propagating, emissive fissure corresponding to Madeleine volcanic alignment. Large white arrows, sector collapse directions, with last events indicated. See discussion in text. (b) E-W topographic profiles across the active volcanic complex of La Grande-Découverte (location in Figure 10). Topography is from topographic maps (1/25 000, IGN), vertical exaggeration: 2. Overall topographic slopes underlined by thin dashed lines with values given in boxes. Black line, Ty fault; U, footwall uplift; D, hanging wall downdrop. Long, black arrows: sector collapse directions with dates.

[49] Another zone with both deep and shallow earthquakes stretches in an ~ENE direction, north of La Désirade graben (Figures 2a and 16). Although the trend of this zone is parallel to that of the graben, the fault plane solutions of several of the shocks show thrust mechanisms on northerly striking planes, implying rupture of the plate interface (Figure 2a). The epicenter of the $M \sim 7.5$, 8 February 1843 earthquake, which destroyed Pointe-à-Pitre [e.g., *Sainte-Claire Deville*, 1843] has been located in the same area (Figures 1 and 2a). The absence of a large tsunami, and of significant vertical deformation along the coastlines of Antigua and Guadeloupe, indeed suggests that

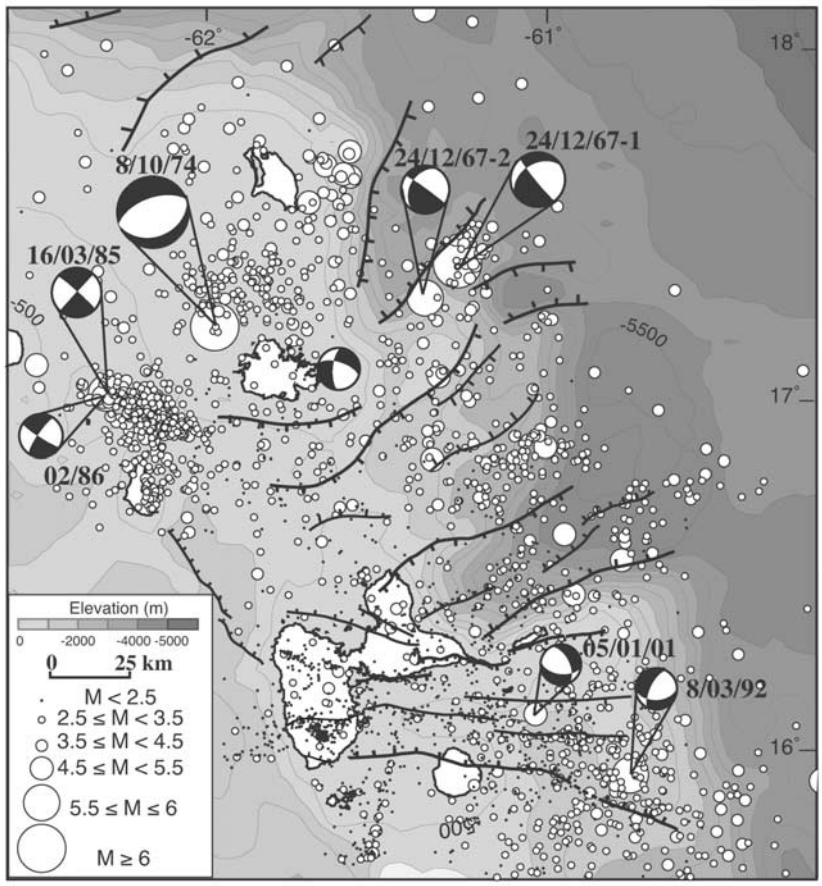

Figure 16. Lesser Antilles arc shallow seismicity (<30 km, 1981–1995) recorded by Guadeloupe and Martinique regional networks (IPGP, see caption of Figure 2b), superimposed to regional active faults map. Faults are from present study and interpretation of overall bathymetry [*Smith and Sandwell*, 1997] (see Figure 17 and text). Focal mechanisms are from Harvard catalog, see caption of Figure 2, and *Stein et al.* [1982].

this large shock might have been an interplate thrust event, deep enough that the rupture did not propagate to the seafloor [*Bernard and Lambert*, 1988].

[50] The dense cluster of shallow seismicity near Montserrat corresponds to the 16 March 1985, M_s = 6.3, Nevis earthquake, with its 3000, $2 \leq M \leq 4.5$ aftershocks [*Girardin et al.*, 1991]. The main event has ruptured a ~30-km-long and 15-km-wide fault segment [e.g., *Girardin et al.*, 1991]. Section D-D′ of Figure 2b, roughly perpendicular to the trend of the cluster, suggests a ~80°N dipping fault plane. The elongation of the aftershock cluster implies that this fault plane strikes ≈WNW (Figure 16). Fault plane solutions for the main shocks and a large aftershock in 1986 are consistent with left-lateral slip on such a steep, NNW striking fault that probably mark the northwestward extension of the Basse-Terre-Montserrat fault system. Such faulting is consistent with ~N-S extension.

[51] In the NNE trending cluster of shallow (≤15 km), $M \geq 3$ earthquakes NE of Antigua, two large consecutive shocks (M_s = 6.3, 24 December (20:03), 1967, and *mb* = 5.9, 24 December (21:32) 1967), show focal mechanisms compatible with normal, right-lateral slip on a northwest dipping, NNE striking fault, also consistent with ~N-S extension.

[52] Finally, two major earthquakes have occurred in the area between Nevis and the Antigua Valley. The first, on 5 April 1690, was felt with intensities of up to IX-X, on many surrounding islands [*Mallet*, 1852]. It is possible that it ruptured the northward extension of the Basse-Terre-Montserrat fault system along the northernmost, Nevis-St Kitts part of the arc (Figure 2a). The second one was the M_s = 7.4, 8 October 1974 Antigua earthquake [*McCann et al.*, 1982]. Both the focal mechanism and the aftershock distribution of this event imply that it ruptured a roughly E-NE striking, southeast dipping normal fault [*McCann et al.*, 1982], roughly parallel to those we mapped near Guadeloupe. That earthquake is therefore also consistent with extension perpendicular to the trench.

6. Summary and Discussion

[53] Our detailed study of young faulting onland and offshore the main islands of the Guadeloupe archipelago helps constrain the active tectonic regime, and its relationship with seismicity and volcanism. The conclusions we reach on the styles and rates of deformation can also be better integrated with overall deformation scenarios of the

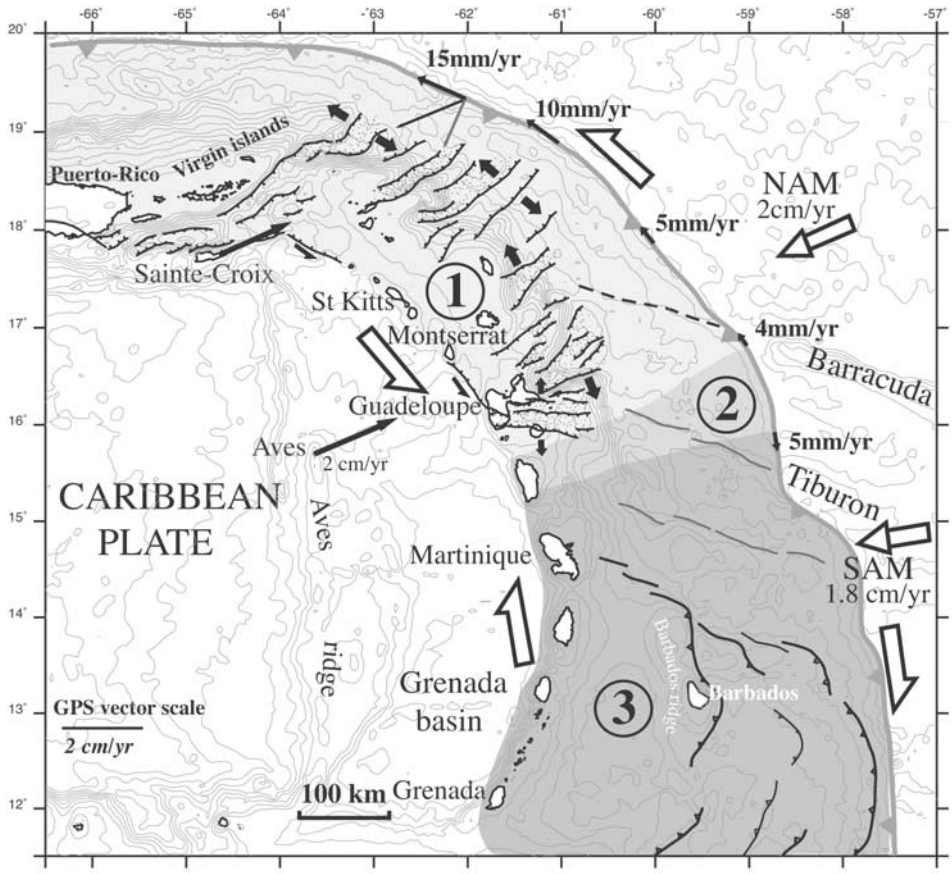

Figure 17. Tectonic model of the Lesser Antilles Arc. 500 m bathymetric contours are from *Smith and Sandwell* [1997]. Faults from Figure 14a and bathymetric contours pattern analysis. Structural interpretation of accretionary prism is based on analysis of bathymetric and topographic contour patterns. Black arrows along the trench: NAM/CAR boundary-parallel slip with rates indicated [*DeMets et al.*, 2000]. Large white arrows: NAM/CAR and SAM/CAR motion vectors from *DeMets et al.* [2000] and *Weber et al.* [2001], respectively. NAM/CAR GPS relative motion vectors measured at Aves and Sainte Croix are indicated [*DeMets et al.*, 2000]. Black double arrows, local direction of extension deduced from fault geometry and distribution. Half black arrows, slip on oblique or strike slip faults. 1, in light gray, zone of sinistral extensional shear; 2-transition zone; 3-in dark grey, zone of dextral oblique thrusting (see discussion in text). White large half arrows indicate sinistral and dextral motion along the trench, respectively.

Caribbean arc, in the framework of new, now well constrained GPS kinematic data at plate scale.

[54] Presently, the leading edge of the arc near Guadeloupe appears to be the site of predominantly trench-parallel extension, as observed in several other orogenic or volcanic arcs in the world (e.g., Tibet [*Armijo et al.*, 1986]; Crete [*Lyon-Caen et al.*, 1988; *Armijo et al.*, 1992]. Such extension gives rise to prominent normal fault and fissure systems that cut either emerged coral platforms, submerged reefs, or volcanic edifices. The faults and fissures trend mostly E-W in the outer part of the arc, and form en echelon arrays that testify to oblique slip where their overall strikes depart from E-W. In the volcanic part of the arc, other, arc parallel normal or oblique faults are found locally. The opening of current tensile cracks range from a few centimeters to a meter. The cumulative throws of the active faults can exceed several hundred meters in rocks that are only a few hundred thousand years old. The most active faults (Gosier, Roche-De-May, Morne-Piton) appear to bound the Marie-Galante graben, which separates the islands of Marie-Galante and Grande-Terre. Slip on such faults appears to be responsible for several historical earthquakes, as well as for current seismicity. Given the lengths of the faults, future earthquake magnitudes could well reach or exceed 6. This implies that the local seismic hazard related to such shallow faults, which are close to the most densely populated areas of the islands, must be investigated and taken seriously, as is that related to larger but more distant earthquakes rupturing the subduction interface. The situation is thus similar to that found along other subduction zones (e.g., Kobe, Japan [e.g., *Toda et al.*, 1998]). The largest fault (Morne-Piton) may slip at a rate of 0.3 to 0.7 mm/yr. The Marie-Galante graben appears to have propagated westward, with its present-day tip lying beneath the most recent volcanic complex of Grande-Découverte-Soufrière. The interaction of the arc-perpendicular graben faults

with other, nearly orthogonal, arc-parallel faults and fissures localized along the volcanic summits, appears to control the volcanic intrusion and extrusion processes in a remarkable way. Volcanic domes and craters are aligned along both directions, but the buttressing effect of the rift shoulders channels blast avalanches to the SW and SE, alternately. The summit of the most recent Soufrière dome (1440 AD) is most prominently cut by an active arc parallel fault-fissure system (Ty fault) which roughly follows the Atlantic-Caribbean water divide and may mark the limit between SW and SE directed sector collapses. Current, down to the east, motion on this fault suggests that the next blast might occur toward Capesterre, on the Atlantic side of the island, rather than toward Basse-Terre, as did the ultimate (3100 B.P.) avalanche.

[55] Another large trough, the Désirade graben, trending about 30° more northerly than the Marie-Galante trough, cuts the outer arc NE of Grande-Terre. Although the two large NNW striking normal faults (Grande-Vigie and Montagne Vercinot) that dissect the northern plateau of Grande-Terre may mark the present termination of the faults that bound that graben to the north, the great Désirade escarpment, to the south, whose cumulative throw (~6 km) is the largest in the Caribbean arc outside the Anegada Passage, does not encroach upon the eastern shore of Grande-Terre. It is likely therefore that this graben is older, and much less active today than a few hundred thousand years ago. It might have once extended farther west, to the more ancient, axial volcanic chain of northern Basse-Terre, across the Grippon plain, prior to deposition of the coral reefs that now cap the northeastern part of the island. The age relationships between the two grabens and the two volcanic complexes of Basse-Terre might thus be comparable, and reflect a similar tectonic-volcanic link. Earthquake fault plane solutions along the northeast stretch of the Désirade graben appear to reflect thrusting on the plate interface rather than arc parallel extension.

[56] The interrelated, active and recent tectonic and volcanic pattern we document near Guadeloupe appears to characterize most of the northern Caribbean arc north of the Island of Dominique (~16°N), and to contrast markedly with that observed along the southern part of the arc. Both can be simply accounted for by kinematic plate interaction.

[57] On extant bathymetric maps [*Smith and Sandwell*, 1997], the northern Caribbean arc is deeply dissected by a series of transverse, ~NE trending troughs (Anegada Passage, Anguilla, Saint Barthélémy and Antigua valleys, Figure 1b) that resemble those of La Désirade and Marie-Galante. Such troughs have a graben-like geometry with steep, facing escarpments bounding flat inner floors that narrow southwestward [*Case and Holcombe*, 1980; *Stefan et al.*, 1985]. Preliminary results from the 1999 R/V *Atalante* (IFREMER) *Aguadomar* marine cruise between Barbuda and Sainte-Lucie, confirm this resemblance and the inference that these troughs are normal fault-bounded grabens, in keeping with the evidence available from the seismicity distribution and earthquake fault plane solutions [e.g., *McCann et al.*, 1982; *Stein et al.*, 1982]. None of the troughs and corresponding normal faults extends west of the volcanic arc. Normal faults south of Antigua appear to meet westward with the Basse-Terre-Montserrat fault system at the Montserrat Soufrière Hills volcano in a manner comparable to that observed at the Soufrière volcano of Basse-Terre.

[58] The southern Caribbean arc south of Martinique shows a different structure (Figures 1 and 17). It is narrower, more continuous, with smaller volcanic islands. The Barbados accretionary prism, fed by sediments from the Orinoco delta, extends as much as 400 km east of the islands with a well developed, 150-km-wide forearc basin. To the north, this accretionary thrust-wedge appears to be bounded by lateral ramps [e.g., *Case and Holcombe*, 1980; *Brown and Westbrook*, 1987], whose positions and trends may be controlled by Atlantic seafloor fabric parallel to the Tiburon and Barracuda ridges. The current deformation of the upper plate south of 15°N is thus characterized by shortening and overthrusting, without sign of arc-parallel extension.

[59] These contrasting tectonic regimes north and south of Dominique cannot easily be accounted for by scenarios proposed to explain extensional faulting above other subduction zones. Although curvature of the arc might induce arc-parallel extension, as inferred for instance in the Marianas [e.g., *Stern and Smoot*, 1998], no such extension is observed south of 15°N.

[60] Hence, such contrasting tectonic regimes and the relatively narrow region in which the deformation pattern changes drastically must be interpreted in term of variable slip partitioning. GPS measurements now constrain the motion of the Caribbean plate relative to both North and South America [*Dixon and Mao*, 1997; *Dixon et al.*, 1998; *DeMets et al.*, 2000; *Weber et al.*, 2001]. They establish that Aves and Sainte-Croix move at $18-20 \pm 3$ mm/yr in an ENE direction relative to North America (Figure 17), confirming predictions made by *Sykes et al.* [1982] and *Deng and Sykes* [1995], rather than by other models [*Jordan*, 1975; *MacDonald and Holcombe*, 1978; *Minster and Jordan*, 1978; *S. Stein et al.*, 1988; *DeMets et al.*, 1990; *Calais and Mercier de Lepinay*, 1993; *DeMets*, 1993]. The resulting parameters (CAR/NAM pole at 64.9°N, 250.5°E, $\omega = 0.214$°/My), together with the results of other GPS campaign that constrain the CAR/SAM motion (pole at 51.5°N, −65.7°E, $\omega = 0.272$°/My), yield a good picture of the interaction between the three plates.

[61] North of 16°N, deformation along the arc is dominated by the interaction between the NAM and Caribbean plate, which entails a trench parallel component of sinistral shear that decreases southeastward from ~15 to ~4 mm/yr seaward of Guadeloupe [*DeMets et al.*, 2000] (Figure 17). Such slip partitioning vanishes south of Guadeloupe or changes sense if the NAM/CAR vector is still used. The SAM/CAR plate motion vector [*Weber et al.*, 2001] south of Dominique is perpendicular to the trench, hence shows no slip-partitioning in the southern part of the arc. We thus interpret shallow seismicity and deformation of the arc north of 15°N to result from NAM/CAR plate motion partitioning [*DeMets et al.*, 2000]. The change in tectonic style and cessation of arc parallel extension south of Dominique probably reflects the vanishing of sinistral slip partitioning. This region may also roughly coincides with the transition from NAM/CAR to SAM/CAR plate motion occurs, although the Barracuda ridge farther north has been suggested to mark the boundary between the NAM and SAM [e.g., *Dixon and Mao*, 1997].

[62] The pattern of faulting observed in and north of Guadeloupe is compatible with sinistral, extensional shear. The normal faults may fan out from the Basse Terre-Montserrat fault system, which parallels the volcanic arc, in a horsetail manner, as commonly observed in regions of oblique extension. Fault plane solutions suggest that the Montserrat fault is left-lateral. This fault, and its possible continuation northward and connection, through en echelon normal faults, with the eastern part of the transpressive Muertos trench or with sinistral faults in Puerto Rico, would thus resemble well known strike-slip faults along oblique subduction zones, which are usually located near the volcanic arc (i.e., Sumatra [e.g., *Sieh et al.*, 1999]; Philippines [e.g., *Barrier et al.*, 1991]). It would stop south of Basse-Terre as CAR/NAM partitioning ceases. Counterclockwise rotation of the blocks separated by the grabens transverse to the northern arc may also absorb some of the trench parallel shear. The dextral fault plane solutions of the 1967 earthquakes along the Antigua valley fault might testify to such rotation. Given the southeast gradient of partitioning, only a half dozen normal faults with slip rates on order of that estimated on the Morne-Piton fault (0.5 ± 0.2 mm/yr) would be necessary to absorb the $\sim$3–4 mm/yr arc parallel strain remaining at the latitude of Guadeloupe.

[63] More detailed strain measurements within and between the islands of the arc, and more accurate surveys of the bathymetry, combined with a better assessment of the crustal seismicity, will be needed to refine and test the tectonic interpretation proposed here, as well as its relationship with volcanism. Some such surveys (e.g., Aguadomar 1999) have already been undertaken, and their results have started to clarify further interaction between the Caribbean and North American plates. A more thorough understanding of this interaction will be essential to improve that of seismic hazard in the Lesser Antilles, as well as perhaps, that of possibly coupled volcanic hazard.

[64] **Acknowledgments.** This work started as part of an effort by the "Département des observatoires" of the Institut de Physique du Globe de Paris to evaluate the earthquake potential of faults in the French Antilles. We are grateful to J. L. Le Mouël, J. L. Cheminée, G. Aubert, and C. Jaupart for their leadership, and to the late J. C. Rossignol, who played a key role in promoting and holding together our research program. We received constant financial support from IPGP, INSU, and CNRS. Particular thanks go to M. Feuillard, J. C. Komorowski, M. Armangon, G. Hamouya, and C. Antenor Habazac. We also benefited from numerous discussions with R. Armijo, G. Boudon, J. Carlut, J. L. Cheminée, B. Meyer, X. Quideleur, M. Semet, B. Villemant. We thank A. Hirn and J. C. Lepine who provided the regional earthquakes location files and H. Got for providing unpublished seismic reflection profiles. We are grateful to J. Weber and an anonymous referee for constructive reviews. This is IPGP contribution 1827.

References

Adamek, S., C. Frohlich, and W. D. Pennington, Seismicity of the Caribbean-Nazca boundary: Constraints on microplate tectonics of the Panama region, *J. Geophys. Res.*, *93*, 2053–2075, 1988.

Andreieff, P., P. Bouysse, and D. Westercamp, Géologie de l'arc insulaire des Petites Antilles et évolution géodynamique de l'Est-Caraïbe, thesis, Univ. de Bordeaux I, Talence, France, 1987.

Armijo, R., P. Tapponnier, J. L. Mercier, and H. Tong-Lin, Quaternary extension in southern Tibet: Field observations and tectonic implications, *J. Geophys. Res.*, *91*, 13,803–13,872, 1986.

Armijo, R., H. Lyon-Caen, and D. Papanastassiou, East-west extension and Holocene normal-fault scarps in the Hellenic arc, *Geology*, *20*, 491–494, 1992.

Armijo, R., B. Meyer, G. C. P. King, A. Rigo, and D. Papanastassiou, Quaternary evolution of the Corinth rift and its implications for the Late Cenozoic evolution of the Aegean, *Geophys. J. Int.*, *126*, 11–53, 1996.

Avouac, J.-P., and G. Peltzer, Active tectonics in southern Xinjiang, China: Analysis of terrace riser and normal fault scarp degradation along the Hotan-Qira fault system, *J. Geophys. Res.*, *98*, 21,773–21,807, 1993.

Barrier, E., P. Huchon, and M. Aurelio, Philippine fault, a key for Philippine kinematics, *Geology*, *19*, 32–35, 1991.

Battistini, R., F. Hinschberger, C. T. Hoang, and M. Petit, La basse terrasse corallienne (Eémien) de la Guadeloupe: Morphologie, datation 230Th/234U, néotectonique, *Rev. Geomorphol. Dyn.*, *35*, 1–10, 1986.

Benedetti, L., P. Tapponnier, G. C. P. King, and L. Piccardi, Surface rupture of the 1857 southern Italian earthquake?, *Terra Nova*, *4*, 206–210, 1999.

Bernard, P., and J. Lambert, Subduction and seismic hazard in the northern Lesser Antilles arc: Revision of the historical seismicity, *Bull. Seismol. Soc. Am.*, *78*, 1965–1983, 1988.

Blanc, F., Corrélation chronologiques et géochimiques des formations volcaniques du sud de la Basse-Terre de Guadeloupe (Petites Antilles): Début du cycle récent, Ph.D. thesis, Univ. Sci. Médic., Grenoble, France, 1983.

Boudon, G., Mécanismes éruptifs et mode de mise en place des dépots d'éruption explosives dirigées: Exemples de la Soufrière (Guadeloupe) et de la Montagne Pelée (Martinique), thesis, Univ. Paris VII-Denis Diderot Univ., France, 1987.

Boudon, G., M. P. Semet, and P. M. Vincent, Flank failure-directed blast eruption at Soufrière, Guadeloupe, French West Indies: A 3000-yr-old Mt., St. Helens?, *Geology*, *12*, 350–353, 1984.

Boudon, G., M. P. Semet, and P. M. Vincent, Magma and hydrothermally driven sector collapses: The 3100 and 11,500 yrs B.P. eruptions of la Grande Découverte (La Soufrière) volcano, Guadeloupe, French West Indies, *J. Volcanol. Geotherm. Res.*, *33*, 317–323, 1987.

Boudon, G., M. P. Semet, and P. M. Vincent, The evolution of la Grande Découverte (La Soufrière) volcano, Guadeloupe (F.W.I.), in *Volcanic Hazards: Assessment and Monitoring*, edited by J. H. Latter, *IAVCEI Proc. Volcanol.*, *1*, 86–109, 1989.

Boudon, G., J. Dagain, M. Semet, and D. Westercamp, Carte et notice explicative de la carte géologique du massif volcanique de la Soufrière (Département de la Guadeloupe, Petites Antilles), scale 1:20,000, Bur. de Rech. Geol. et Min., Orléans, France, 1990.

Boudon, G., M. P. Semet, and P. M. Vincent, Les éruptions à écroulement de flanc sur le volcan de la Grande-Découverte (La Soufrière) de Guadeloupe: Implication sur le risque volcanique, *Bull. Soc. Geol. Fr.*, *163*, 159–167, 1992.

Bouysse, P., Caractères morphostructuraux et évolution géodynamique de l'arc insulaire des Petites Antilles (Campagne Arcante 1), *Bull. Bur. Rech. Geol. Min. Fr.*, *2*, 185–210, 1979.

Bouysse, P., and F. Garrabé, Evolution tectonique néogène des îles calcaires de l'archipel de la Guadeloupe, *C. R. Acad. Sci., Ser. II*, *298*, 763–766, 1984.

Bouysse, P., and P. Guennoc, Données sur la structure de l'arc insulaire des Petites Antilles: Entre St Lucie et Anguilla, *Mar. Geol.*, *53*, 131–166, 1983.

Bouysse, P., and D. Westercamp, Subduction of Atlantic aseismic ridges and late Cenozoic evolution of the Lesser Antilles island arc, *Tectonophysics*, *175*, 349–380, 1990.

Bouysse, P., S. Robert, P. Guennoc, and S. Monti, Bathymétrie détaillée (SeaBeam) et anomalies magnétiques dans les Antilles françaises: Interprétation morphostructurale de la vallée de la Désirade et des côtes occidentales de Basse-Terre de Guadeloupe et de Martinique (Campagne ARCANTE 2- THERMOSITE, NO Jean Charcot, Décembre 1980), *Doc. B. R. G. M.*, *63*, 78, 1983a.

Bouysse, P., R. Schmidt-Effing, and D. Westercamp, La Désirade Island (Lesser Antilles) revisited: Lower Cretaceous radiolarian cherts and arguments against an ophiolitic origin for the basal complex, *Geology*, *11*, 244–247, 1983b.

Bouysse, P., P. Andreieff, M. Richard, J. C. Baubron, A. Mascle, R. C. Maury, and D. Westercamp, Géologie de la ride d'Aves et des pentes sous marines du nord des Petites Antilles, esquisse bathymétrique à 1:1,000,000 de l'est-caraïbe, *Doc. B. R. G. M.*, *93*, 141 pp., 1984.

Bouysse, P., D. Westercamp, P. Andreiff, J. C. Baubron, and G. Scolari, Le volcanisme néogène récent au large des côtes Caraïbes des Antilles Françaises: Relations avec le volcanisme à terre et évolution du front volcanique, *Geol. Fr.*, *1*, 101–114, 1985.

Bouysse, P., A. Mascle, A. Mauffret, B. Mercier de Lepinay, I. Jany, A. Leclere-Vanhoeve, and M. C. Montjaret, Reconnaissance de structures tectoniques et volcaniques sous marines de l'arc des Petites Antilles (Kick'em Jenny, Qualibou, Montagne Pelée, Nord-ouest de la Guadeloupe), *Mar. Geol.*, *81*, 261–287, 1988.

Bouysse, P., F. Garrabé, T. Mauboussin, P. Andreieff, R. Battistini, P. Carlier, F. Hinschberger, and J. Rodet, Carte géologique département de la Guadeloupe: Marie-Galante et îlets de la Petite-Terre, scale 1:50,000, Bur. de Rech. Geol. et Min., Paris, 1993.

Brown, K. M., and G. K. Westbrook, The tectonic fabric of the Barbados Ridge accretionary complex, *Mar. Pet. Geol.*, *4*, 71–81, 1987.

Calais, E., and B. Mercier de Lepinay, Semiquantitative modeling of strain and kinematics along the Caribbean/North America strike-slip plate boundary zone, *J. Geophys. Res.*, *98*, 8293–8308, 1993.

Carlut, J., X. Quidelleur, V. Courtillot, and G. Boudon, Paleomagnetic directions and K/Ar dating of 0 to 1 Ma lava flows from La Guadeloupe Island (French West Indies): Implications for time-averaged field models, *J. Geophys. Res.*, *105*, 835–849, 2000.

Case, J. E., and T. L. Holcombe, Geologic-tectonic map of the Caribbean region, scale 1:2,500,000, *U.S. Geol. Surv. Misc. Invest. Ser., Map, I–1100*, 1980.

Chabellard, J. G., Cadre géodynamique et néotectonique des Petites Antilles, Étude Bibliographique, *Rep. D. R. M.*, Orleans, France, 1986.

Dagain, J., La mise en place du massif de la Madeleine-Soufrière, basse-terre de Guadeloupe, Antilles, thesis, Univ. Paris XI-Paris Sud, Orsay, France, 1981.

DeMets, C., Earthquake slip vectors and estimates of present-day plate motions, *J. Geophys. Res.*, *98*, 6703–6714, 1993.

DeMets, C., R. G. Gordon, D. F. Argus, and S. Stein, Current plate motions, *Geophys. J. Int.*, *101*, 425–478, 1990.

DeMets, C., P. E. Jansma, G. S. Mattioli, T. H. Dixon, F. Farina, R. Bilham, E. Calais, and P. Mann, GPS geodetic constraints on Caribbean-North America plate motion, *Geophys. Res. Lett.*, *27*, 437–440, 2000.

Deng, J., and L. R. Sykes, Determination of Euler pole for contemporary relative motion of Caribbean and North American plates using slip vectors of interplate earthquakes, *Tectonics*, *14*, 39–53, 1995.

De Reynal de Saint Michel, A., Carte géologique détaillée de la France: Département de la Guadeloupe, Feuille de Grande-Terre, scale 1:50,000, Minist. de l'Ind., Paris, 1961.

De Reynal de Saint Michel, A., Carte géologique détaillée de la France: Département de la Guadeloupe, Feuille de Basse-Terre et des Saintes, scale 1:50,000, Minist. de l'Ind., Paris, 1966.

Dixon, T. H., and A. Mao, A GPS estimate of relative motion between North and South America, *Geophys. Res. Lett.*, *24*, 535–538, 1997.

Dixon, T. H., F. Farina, C. DeMets, P. Jansma, P. Mann, and E. Calais, Relative motion between the Caribbean and North American plates and related boundary zone deformation from a decade of GPS observations, *J. Geophys. Res.*, *103*, 15,157–15,182, 1998.

Dorel, J., Seismicity and seismic gap in the Lesser Antilles arc and earthquake hazard in Guadeloupe, *Geophys. J. R. Astron. Soc.*, *67*, 679–695, 1981.

Dorel, J., S. Eschenbrenner, and M. Feuillard, Contribution à l'étude sismique de l'arc des Petites Antilles, *Ann. Geophys.*, *27*, 295–302, 1971.

Dziewonski, A. M., G. Ekstrom, and N. N. Maternovskaya, Centroid-moment tensor solutions for October–December, 1999, *Phys. Earth Planet. Int.*, *121*, 205–221, 2000.

Feuillard, M., Macrosismicité de la Guadeloupe et de la Martinique, report, Instit. de Phys. du Globe de Paris, 1985.

Feuillet, N., Sismotectonique des Petites Antilles. Liaison entre activité sismique et volcanique, thesis, Univ. Paris VII-Denis Diderot Univ., France, 2000.

Feuillet, N., I. Manighetti, and P. Tapponnier, Active extension perpendicular to subduction in the Lesser Antilles island arc; Guadeloupe, French Antilles (in French), *C. R. Acad. Sci., Ser. II*, *333*(9), 583–590, 2001.

Flinch, J., V. Rambaran, W. Ali, V. De Lisa, G. Hernandez, K. Rodrigues, and R. Sams, Structure of Gulf of Paria pull-apart basin (eastern Venezuela-Trinidad), in *Caribbean Basins*, edited by P. Mann, pp. 477–494, Elsevier Sci., New York, 1999.

Gadalia, A., and D. Westercamp, Prospection géothermique de la région de Bouillante-Vieux Habitants, Guadeloupe, *Rep. 84 SGN 063 GTH*, Bur. de Rech. Geol. et Min., Orléans, France, 1984.

Garrabé, F., P. Andreieff, P. Bouysse, and J. Rodet, Notice explicative de la carte géologique de Grande-Terre: Département de la Guadeloupe, scale 1:50,000, Bur. de Rech. Geol. et Min., Orléans, France, 1988.

Gérard, A., D. Westercamp, P. Bouysse, G. Dubreuil, and J. Varet, Etude géophysique préliminaire à une évaluation du potentiel géothermique des Antilles françaises (Martinique, Guadeloupe), *Doc. B. R. G. M.*, *27*, 40 pp., 1981.

Girardin, N., M. Feuillard, and J. P. Viode, Réseau régional sismique de l'arc des Petites Antilles: Sismicité superficielle (1981–1988), *Bull. Soc. Geol. Fr.*, *162*, 1003–1015, 1991.

Got, H., J. C. Aloïsi, H. Inoubli, M. Perret, and L. Mirabile, Etude structuro-sédimentaire des marges sud et ouest de la Guadeloupe, in *Géodynamique des Caraïbes*, edited by A. Mascle, pp. 161–172, Technip, Paris, 1985.

Grellet, B., B. Sauret, J. G. Chabellard, and J. R. Bonneton, Cadre général de la tectonique récente de la Guadeloupe, *Rep. 88 SNG 627 GEG*, Bur. de Rech. Geol. et Min., Orléans, France, 1988.

Heubeck, C., and P. Mann, Geologic evaluation of the plate kinematic models for North American-Caribbean plate boundary zone, *Tectonophysics*, *191*, 1–26, 1991.

Holcombe, T. L., J. W. Ladd, G. Westbrook, T. Edgar, and C. L. Bowland, Caribbean marine geology and basins of the plate interior, in *The Geology of North America*, vol. H, *The Caribbean Region*, edited by G. Dengo and J. E. Case, pp. 231–260, Geol. Soc. of Am., Boulder, Colo., 1990.

Inoubli, H., Contribution à l'étude structuro-sédimentaire des fonds entre la Guadeloupe et Marie-Galante (Petites Antilles), DEA report, Univ. of Perpignan, France, 1981.

Jordan, T. H., The present-day motions of the Caribbean plate, *J. Geophys. Res.*, *80*, 4433–4439, 1975.

Lasserre, G., La Guadeloupe, thesis, Univ. de Bordeaux I, Talence, France, 1961.

Le Mouël, J. L., J. P. Pozzi, J. C. Rossignol, and M. Feuillard, Levé aéromagnétique de l'archipel de la Guadeloupe: Description et implications tectoniques, *Bull. Soc. Geol. Fr.*, *21*, 135–148, 1979.

Lyon-Caen, H., et al., The 1986 Kalamata (South Peloponnesus) earthquake: Detailed study of a normal fault, evidence for east-west extension in the Hellenic Arc, *J. Geophys. Res.*, *93*, 14,967–15,000, 1988.

MacDonald, K. C., and T. L. Holcombe, Inversion of magnetic anomalies and sea-floor spreading in the Cayman Trough, *Earth Planet. Sci. Lett.*, *40*, 407–414, 1978.

Mallet, R., Catalogue of recorded earthquakes, in *Third Report on the Facts of Earthquake Phenomena*, pp. 1–326, British Assoc. for the Adv. of Sci., London, 1852.

Manighetti, I., P. Tapponnier, V. Courtillot, S. Gruszow, and P.-Y. Gillot, Propagation of rifting along the Arabia-Somalia plate boundary: The Gulfs of Aden and Tadjoura, *J. Geophys. Res.*, *102*, 2681–2710, 1997.

Manighetti, I., P. Tapponnier, P.-Y. Gillot, E. Jacques, V. Courtillot, R. Armijo, J. C. Ruegg, and G. C. P. King, Propagation of rifting along the Arabia-Somalia plate boundary: Into Afar, *J. Geophys. Res.*, *103*, 4947–4974, 1998.

Mann, P., F. W. Taylor, R. L. Edwards, and T.-L. Ku, Actively evolving microplate formation by oblique collision and sideways motion along strike-slip-faults: An example from the the northeastern Caribbean plate margin, *Tectonophysics*, *246*, 1–69, 1995.

Mascle, A., and P. Letouzey, Geological map of the Caribbean, Technip, Paris, 1990.

McCann, W. R., On the earthquake hazards of Puerto Rico and the Virgin Islands, *Bull. Seismol. Soc. Am.*, *75*, 251–262, 1985.

McCann, W. R., J. W. Dewey, A. J. Murphy, and S. T. Harding, A large normal-fault earthquake in the overriding wedge of the Lesser Antilles subduction zone: The earthquake of 8 October 1974, *Bull. Seismol. Soc. Am.*, *72*, 2267–2283, 1982.

Mervoyer, B., Volcanisme récent et actuel de la Basse-Terre: Le massif de la Soufrière, paper presented at VIIème Conférence Géologique des Caraïbes, Bur. de Rech. Géol. et Minières, Guadeloupe, French West Indies, 1974.

Minster, J. B., and T. H. Jordan, Present-day plate motions, *J. Geophys. Res.*, *83*, 5331–5354, 1978.

Montgomery, H., E. A. Passagno, and Y. M. Munoz, Jurassic (Tithonian) radiolaria from la Désirade (Lesser Antilles): Preliminary paleontological and tectonic implications, *Tectonics*, *11*, 1426–1432, 1992.

Pindell, J. L., and S. F. Barrett, Geological evolution of the Caribbean region, in *The Geology of North America*, vol. H, *The Caribbean Region*, edited by G. Dengo and J. E. Case, pp. 405–432, Geol. Soc. of Am., Boulder, Colo., 1990.

Polyak, B. G., et al., Evidence of submarine hydrothermal discharge to the northwest of Guadeloupe Island (Lesser Antilles island arc), *J. Volcanol. Geotherm. Res.*, *54*, 81–105, 1992.

Robson, G., An earthquake catalog for the eastern Caribbean 1530–1960, *Bull. Seismol. Soc. Am.*, *54*, 785–832, 1964.

Sainte-Claire Deville, C., Observations sur le tremblement de terre éprouvé à la Guadeloupe le 8 février 1843, Imprimerie du Gouverneur, Basse-Terre, Juillet 1843.

Sieh, K., S. N. Ward, D. Natawidjaja, and B. M. Suwargadi, Crustal deformation at the Sumatran subduction zone revealed by coral rings, *Geophys. Res. Lett.*, *26*, 3141–3144, 1999.

Smith, W. H. F., and D. T. Sandwell, Global sea floor topography from satellite altimetry and ship depth sounding, *Science*, *277*, 1956–1962, 1997.

Stefan, J. F., R. Blanchet, and B. Mercier de Lepinay, Les festons nord et sud caraïbes (Hispaniola-Porto Rico; Panama et Colombie-Venezuela): Des pseudo-subductions induites par le raccourcissement est-ouest du bâti continental péri-caraïbe, in *Symposium sur la Géodynamique des Caraïbes*, pp. 35–51, Technip, Paris, 1985.

Stein, R. S., G. C. P. King, and J. B. Rundle, The growth of geological structures by repeated earthquakes, 2, Field examples of continental dip-slip faults, *J. Geophys. Res.*, *93*, 13,319–13,331, 1988.

Stein, R. S., P. Briole, J. C. Ruegg, P. Tapponnier, and F. Gasse, Contemporary, Holocene, and Quaternary deformation of the Asal rift, Djibouti: Implications for the mechanics of slow spreading ridges, *J. Geophys. Res.*, *96*, 21,789–21,806, 1991.

Stein, S., J. F. Engeln, D. A. Wiens, K. Fujita, and R. C. Speed, Subduction seismicity and tectonics in the Lesser Antilles arc, *J. Geophys. Res.*, *87*, 8642–8664, 1982.

Stein, S., C. DeMets, R. G. Gordon, J. Brodholt, D. Argus, J. F. Engeln, P. Lundgren, C. Stein, D. A. Wiens, and D. F. Woods, A test of alternative Caribbean plate relative motion models, *J. Geophys. Res.*, *93*, 3041–3050, 1988.

Stern, R. J., and C. Smoot, A bathymetric overview of the Mariana forearc, *Island Arc*, *7*, 525–540, 1998.

Sykes, L. R., and M. Ewing, The seismicity of the Caribbean region, *J. Geophys. Res.*, *70*, 5065–5074, 1965.

Sykes, L. R., W. R. McCann, and A. L. Kafka, Motion of the Caribbean plate during last 7 million years and implications for earlier Cenozoic movements, *J. Geophys. Res.*, *87*, 10,656–10,676, 1982.

Toda, S., R. S. Stein, P. A. Reasenberg, J. H. Dieterich, and A. Yoshida, Stress transferred by the 1995 *Mw* = 6.9 Kobe, Japan, shock: Effect on aftershocks and future earthquake probabilities, *J. Geophys. Res.*, *103*, 24,543–24,565, 1998.

Tomblin, J. F., Seismicity and plate tectonics in the eastern Caribbean, in *Transaction of the Caribbean Geological Conference, Memorias Conferencia Geological del Caribe*, vol. 6, pp. 277–282, Queens Coll., Flushing, N. Y., USA, 1972.

Wallace, R. E., Active faults, palaeoseismology, and earthquake hazards in the western United States, in *Earthquake Prediction: An International Review, Maurice Ewing Ser.*, vol. 4, edited by D. W. Simpson and P. G. Richards, pp. 209–216, AGU, Washington, D. C., 1981.

Weber, J. C., T. H. Dion, C. DeMets, W. B. Ambeh, P. Jansma, G. Mattioli, J. Saleh, G. Sella, R. Bilham, and O. Perez, GPS estimate of relative motion between the Caribbean and South American plates, and geologic implications for Trinidad and Venezuela, *Geology*, *29*, 75–78, 2001.

Westercamp, D., Notice explicative de la carte géologique de la Désirade: Département de la Guadeloupe, scale 1:25,000, Bur. de Rech. Geol. et Min., Orléans, France, 1980.

Westercamp, D., and H. Tazieff, *Guides géologiques régionaux, Martinique, Guadeloupe, St Martin, La Désirade*, 135 pp., Masson, Paris, 1980.

N. Feuillet, Istituto Nazionale di Geofisica e Vulcanologia, Via di Vigna Murata, 605, I-00143 Rome, Italy. (feuillet@ingv.it)

I. Manighetti and P. Tapponnier, Institut de Physique du Globe de Paris, Laboratoire de Tectonique et Mécanique de la Lithosphère, CNRS UMR 7578, 4 Place Jussieu, F-75252 Paris Cedex 05, France.

E. Jacques, Institut de Physique du Globe de Strasbourg, UMR CNRS 7516, 5 rue Rene Descartes, F-67084 Strasbourg, France.